Collagen (I) homotrimer potentiates the osteogenesis imperfecta (oim) mutant allele and reduces survival in male mice

Katie J. Lee [a], Lisa Rambault [b], George Bou-Gharios [a], Peter D. Clegg [a, c], Riaz Akhtar [d], Gabriela Czanner [e], Rob van 't Hof [a], Elizabeth G. Canty-Laird [a, c]

[a] Department of Musculoskeletal and Ageing Science, Institute of Life Course and Medical Sciences, University of Liverpool, William Henry Duncan Building, 6 West Derby Street, Liverpool, L7 8TX, United Kingdom

[b] Université de Poitiers, France

[c] The Medical Research Council Versus Arthritis Centre for Integrated Research into Musculoskeletal Ageing (CIMA)

[d] Department of Mechanical, Materials and Aerospace Engineering, School of Engineering, University of Liverpool, L69 3GH, United Kingdom

[e] School of Computer Science and Mathematics, Faculty of Engineering and Technology, Liverpool John Moores University, Byrom Street, Liverpool, L3 3AF, United Kingdom

Abstract

Type I collagen is the major structural component of bone where it exists as an $(\alpha1)_2(\alpha2)_1$ heterotrimer in all vertebrates. The osteogenesis imperfecta (oim) mouse model comprising solely homotrimeric $(\alpha1)_3$ type I collagen, due to a dysfunctional α2 chain, has a brittle bone phenotype implying that the heterotrimeric form is required for physiological bone function. However, humans with rare null alleles preventing synthesis of the α2 chain have connective tissue and cardiovascular abnormalities (cardiac valvular Ehlers Danlos Syndrome), without evident bone fragility. Conversely a prevalent human single nucleotide polymorphism leading to increased homotrimer synthesis is associated with osteoporosis. Whilst the oim line is well-studied, whether homotrimeric type I collagen is functionally equivalent to the heterotrimeric form in bone has not been demonstrated. Col1a2 null and oim mouse lines were used in this study and bones analysed by microCT and 3-point bending. RNA was also extracted from heterozygote tissues and allelic discrimination analyses performed using qRT-PCR. Here we comprehensively show for the first time that mice lacking the α2(I) chain do not have impaired bone biomechanical or structural properties, unlike oim homozygous mice. However Mendelian inheritance was affected in male mice of both lines and male mice null for the α2 chain exhibited age-related loss of condition. The brittle bone phenotype of oim homozygotes could result from detrimental effects of the oim mutant allele, however, the phenotype of oim heterozygotes is known to be less severe. We used allelic discrimination to show that the oim mutant allele is not downregulated in heterozygotes. We then tested whether gene dosage was responsible for the less severe phenotype of oim heterozygotes by generating compound heterozygotes. Data showed that compound heterozygotes had impaired bone structural properties as compared to oim heterozygotes, albeit to a lesser extent than oim homozygotes. Hence, we concluded that the presence of heterotrimeric collagen-1 in oim heterozygotes alleviates the effect of the oim mutant allele but a genetic interaction between homotrimeric collagen-1 and the oim mutant allele leads to bone fragility.

Key words: collagen, homotrimer, Col1a2, α2(I), osteogenesis imperfecta, cvEDS

Introduction

Type I collagen is the major structural component of vertebrate tissues, where it exists as insoluble fibrils formed from arrays of trimeric collagen molecules. In tetrapods, type I collagen molecules are predominantly $(\alpha1)_2(\alpha2)_1$ heterotrimers derived from the polypeptide gene products of the Col1a1 and Col1a2 genes. Trimeric type I procollagen molecules contain a central triple-helical domain flanked by globular N- and C-propeptide regions, that are proteolytically removed to facilitate fibrillogenesis (1). Procollagen molecules are synthesised in the endoplasmic reticulum of the secretory pathway where individual molecules first associate via the C-propeptides. C-propeptide association facilitates chain registration and folding of the triple helical domain into a right-handed triple helix. The type-specific assembly of fibrillar procollagens has been attributed to defined amino acid sequences within the C-propeptide including a chain recognition sequence (2), specific stabilising residues (3) and a cysteine code (4), although none fully explain the preferential heterotrimerisation of type I procollagen.

Abnormal type I collagen $(\alpha1)_3$ homotrimer, derived from COL1A1 alone, is genetically or biochemically associated with common age-related human diseases including osteoporosis (5), osteoarthritis (6-8), intervertebral disc degeneration (9), arterial stiffening (10), cancer (11), liver fibrosis (12) and Dupuytren's contracture (13). The homotrimeric form is resistant to mammalian collagenases (14) and alterations in collagen crosslinking have been reported in the osteogenesis imperfecta murine (oim) model, which lacks a functional α2(I) chain (15-17). Hence the presence of homotrimeric collagen (I) in human disease may alter the ability of tissues to respond to changing physiological demands by slowing remodelling and altering tissue mechanics.

The oim mutation is a deletion of a single guanidine residue, causing a frameshift that alters the last 47 amino acids, and reportedly adds an additional residue to the α2 chain of type I procollagen (Fig. 1A). The mutant α2 chain cannot be incorporated into trimers hence giving rise to solely homotrimeric collagen-1 in oim homozygotes. Homozygous oim/oim mice have osteopenia, progressive skeletal deformities, spontaneous fractures, cortical thinning and small body size (18) with corresponding alterations to bone structure and material properties (19, 20). Homozygous oim mice also have a reduced circumferential breaking strength and greater compliance of aortae (16, 21), reduced ultimate stress and strain tendon for tendon (22) and kidney glomerulopathy (23).

The oim mutation is very similar to the first-identified mutation causing human osteogenesis imperfecta (autosomal recessive Silence type III), in which a 4 nucleotide deletion (c.4001_4004del) causes a frameshift (p.(Asn1334Serfs*34)) to alter the last 33 amino acids of the α2 chain of type I procollagen (Pihlajaniemi et al., 1984). The human mutation also results in homotrimeric type I collagen synthesis as the defective α2(I) chain cannot be incorporated into trimers (24, 25). In two additional patients with mild osteogenesis imperfecta, novel mutations were identified causing a 48 amino acid truncation of the α2 chain and a substitution of a cysteine residue important for interchain disulphide bonding respectively (26). In these cases the α2 chain was again synthesised but not incorporated into trimers. A similar mutation causing severe osteogenesis imperfecta in a Beagle dog was caused by a heterozygous 9 nucleotide replacement of a 4 nucleotide stretch, leading to a 37 residue truncation of the α2 chain and alteration of the final 44 amino acids of the truncated polypeptide (Campbell et al., 2001).

Oim heterozygotes do not show spontaneous fractures but appear to have a bone phenotype intermediate between that of wild-type and homozygous mice (20, 27-29). Similarly the parents of the human proband had no history or evidence of fractures but had a marked decrease in bone mass (30).

The osteogenesis imperfecta brittle bone phenotype, and the genetic association of collagen (I) homotrimer with osteoporosis (5, 31) contrasts with the phenotype of human patients in which

mutations leading to nonsense-mediated decay of the COL1A2 mRNA cause a specific cardiac valvular form of Ehlers-Danlos syndrome (cv-EDS), not involving bone (32, 33) and evidence that Col1a2 silencing does not affect *in vitro* osteoblast mineralisation (34). EDS is generally characterised by hyperextensible skin and joint hypermobility. In cv-EDS patients the α2 chain of type I collagen is not synthesised, therefore all type I collagen molecules would be homotrimeric. It has been hypothesised that the phenotypic differences between the OI and cv-EDS patients could be explained by the cellular stress elicited by the presence of misfolded α2(I) procollagen chains in osteogenesis imperfecta (26, 35, 36), having a particularly detrimental effect on bone. Cellular stress has been implicated in human osteogenesis imperfecta caused by substitutions in the C-propeptide of the α-1(I) chain (37), in mouse models of triple-helical region mutations; Aga2 (90 a.a. extension to the α1(I) chain) (38), Brtl IV (G349C in α1(I)) (39) and Amish (G610C in α2(I)), identical to that found in a human kindred) (40), as well as in the zebrafish model Chihuahua (G574D in α1(I)) (41).

In this study we compared the bone phenotype of the oim model to that of a Col1a2 null mouse. We considered that comparing the oim model to that of a Col1a2 null line provided a unique opportunity to distinguish between the intracellular and extracellular effects of a collagen mutation linked to brittle bone disease, as well as to elucidate the effect of collagen (I) homotrimer on bone structure and mechanics. Specifically, we compared the bone phenotype of oim homozygous and heterozygous mutant mice with that of mice containing 1 or 2 copies of a targeted Col1a2 null allele and wild-type controls, in order to determine the contribution of collagen (I) homotrimer to bone fragility.

Results

Tm1b homozygotes lack the α2(I) collagen chain in bone and tendon

To verify lack of the α2(I) chain in tm1b homozygotes, tendon and bone samples from 8 week old mice were labelled with [14C]proline to detect newly synthesised collagen (I). SDS-PAGE analysis of labelled tissue extracts verified lack of α2(I) chain synthesis in tail tendon, bone and patellar tendon (Fig. 1C).

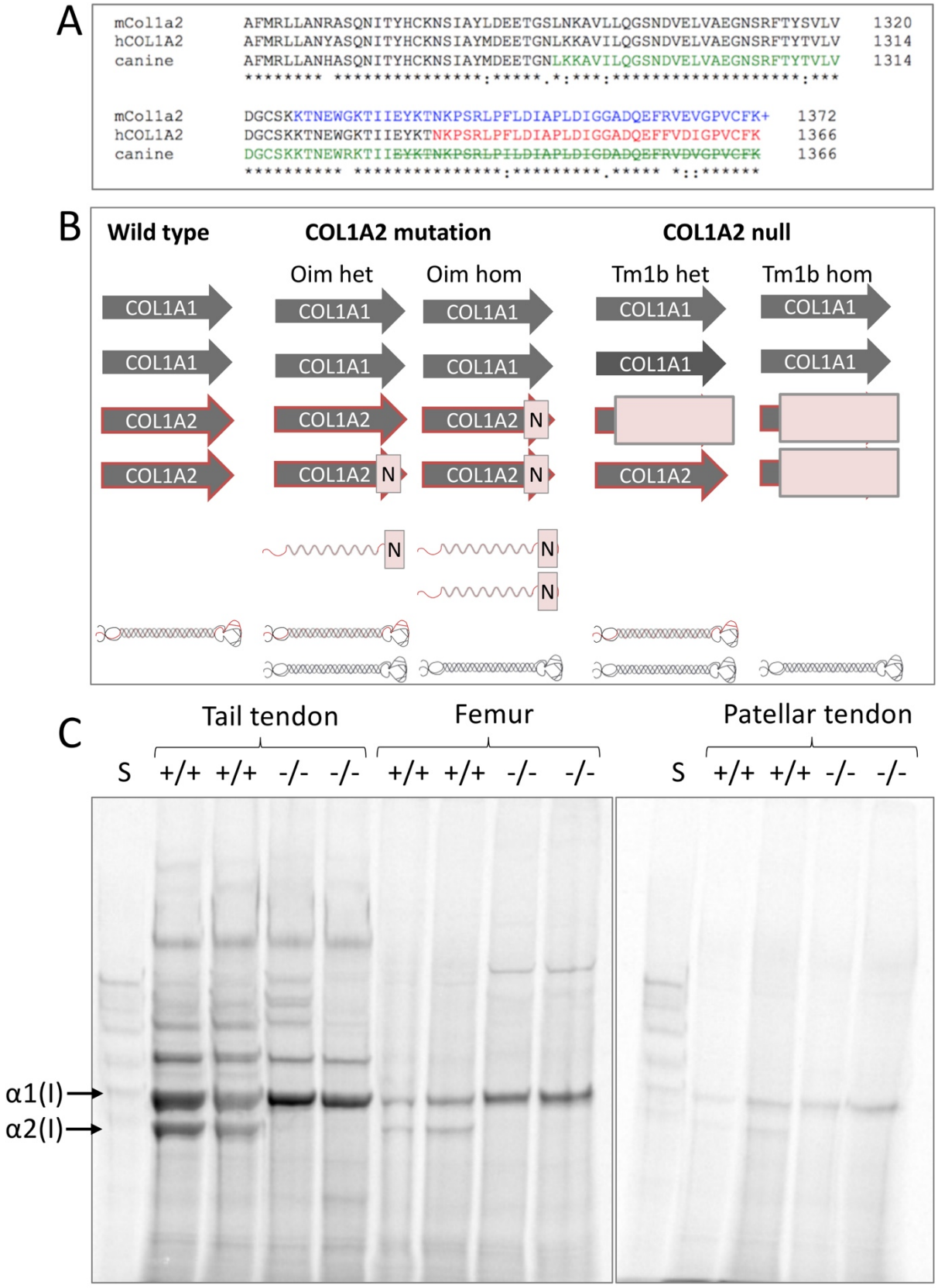

Figure 1. Col1a2 mutant and null alleles. A: Amino acid sequence alignment for the final 112 residues of the mouse (mCol1a2), human (hCOL1A2) and canine α2(I) collagen chains. Colour change indicates amino acid sequence changed from that shown due to frameshift caused by the oim or equivalent

126 mutation. + indicates reported additional amino acid (18). Strike-through indicates truncation. B:
127 Genetic differences between the oim and Col1a2 null lines with implications for collagen (I) protein
128 synthesis. Arrows indicate COL1 genes; N indicates mutation, light red box indicates null allele. Folded
129 heterotrimeric proteins are indicated in black and red, whilst homotrimers are in black only. The
130 presence of unincorporated mutant Col1a2 allele is indicated as a red waveform with a mutation (N). C:
131 Tendon and bone tissue from Tm1b wild-type (+/+) and homozygote (-/-) mice were labelled with
132 [14C]proline and analysed by delayed reduction SDS-PAGE. No labelled α2(I) chain was present in tm1b
133 homozygotes (-/-) unlike in wild-type controls (+/+) indicating that tm1b homozygotes are Col1a2 null.
134 S; collagen standard. α1(I) and α2(I) chains are indicated.
135
136 **Alterations to Mendelian inheritance in male mice of the oim and Col1a2 null lines**
137 To determine if either the oim or Col1a2 alleles resulted in loss of mice prior to weaning, a chi-squared
138 test was performed on genotype data for Col1a2 null and oim mice. There were significant differences
139 between the observed and expected genotype percentages for male mice of both lines (oim; p=0.01,
140 Col1a2 null; p=0.033), whereas no differences were seen for female mice of either line (Fig. 2 A-B). For
141 oim males there was an 10.0% increase in wild-types, a 6.2% decrease in heterozygotes and a 3.8%
142 decrease in homozygotes; whereas for Col1a2 null males there was an 8.0% increase in wild-types, a
143 9.6% decrease in heterozygotes and a 1.6% increase in homozygotes. Hence increased numbers of male
144 wild-types and reduced numbers of male heterozygotes were observed for both lines. Conversely the
145 data supported Mendelian inheritance in female mice.
146
147 **Spontaneous fractures were observed solely in oim homozygotes, whilst male Col1a2 null**
148 **homozygotes exhibited mild joint swelling.**
149 During colony maintenance it was noticeable that spontaneous fractures occurred in the oim line, but
150 not in the Col1a2 null line. Mildly swollen ankle joints were however observed in male tm1b mice which
151 was initially attributed to fighting. The proportion of mice with swollen joints, or noticeable fractures
152 with swelling were determined, including those requiring analgesia (Fig. 2 C-D). Male mice
153 demonstrated a more severe phenotype than female mice for both the Col1a2 null and oim lines. For
154 the oim line fractures and associated swelling were observed in homozygous mice only, with an
155 incidence of 47% for males (20 out of 43) and 20% (10 out of 50) for females. 26% of male mice (11 out
156 of 43) and 18% of female mice (9 out of 50) received analgesic medication. Swollen joints alone
157 presented in 6% of male oim heterozygotes (5 out of 89), 2% of male oim homozygotes (1 out of 43)
158 and 2% of female oim homozygotes (1 out of 50). For the Col1a2 null line no bone fractures were
159 observed and no analgesia was required to be administered. Swollen joints were observed
160 predominantly in male homozygotes with an incidence of 23% (19 out of 83). Less than 4% of male wild-
161 type (4 out of 103), heterozygous (4 out of 126) and female homozygous (1 out of 56) mice presented
162 with swollen joints. No female wild-type or heterozygous mice were reported to have swollen joints.
163 For mouse weights recorded after euthanasia at 18 weeks, male and female oim homozygotes were
164 22.7% and 20.0% lighter than wild-types (Fig. 2E). Heterozygotes were of intermediate weight with
165 male homozygotes being 17.1% lighter than male heterozygotes and female heterozygotes being 13.6%
166 lighter than wild-types. In contrast, there were no significant differences in weight between genotypes
167 for the Col1a2 null line (Fig. 2F).
168

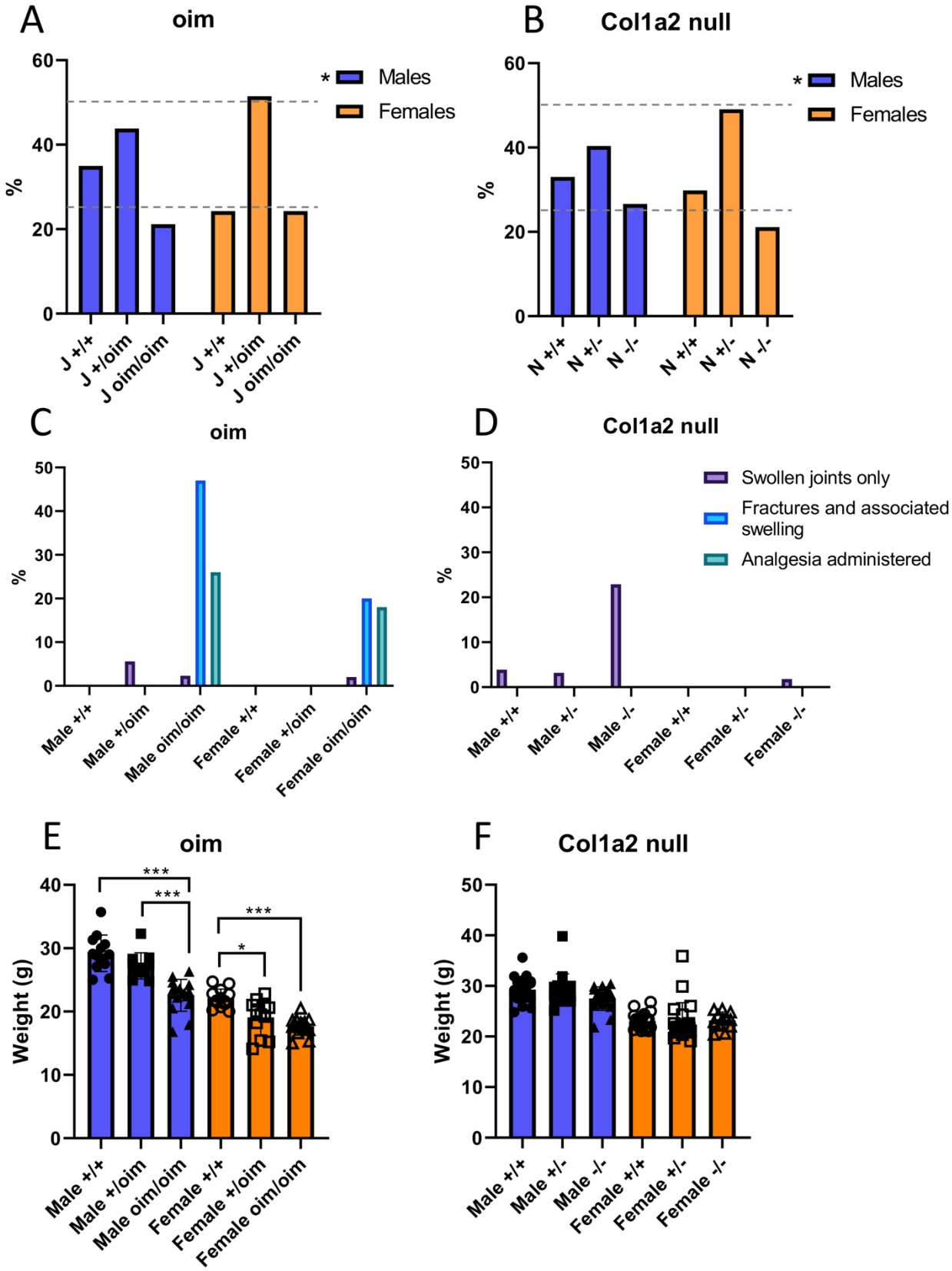

Figure 2. Inheritance pattern, musculoskeletal health summary and mouse weights for the oim and Col1a2 null lines. A-B: The percentage of mice of each genotype born to heterozygous parents for the oim (A) and Col1a2 null (B) lines. A chi-squared test showed significant differences between observed inheritance and expected Mendelian inheritance (25%, 50%, 25%; dashed grey lines) for male mice of both lines. C-D: The number of mice suffering from swollen joints and bone fractures as well as those

treated with analgesics were recorded for the oim (C) and Col1a2 null (D) lines. These numbers are expressed as a percentage of total mouse numbers. A-D: n=71, 89 and 43 for male oim +/+, +/oim and oim/oim mice respectively; n=50, 106 and 50 for female oim +/+, +/oim and oim/oim mice respectively; n= 103, 126 and 83 for male Col1a2 null +/+, +/-, -/- mice respectively and; n=79, 130, 56 for female Col1a2 null +/+, +/-, -/- mice respectively. Swollen joints were mild in the Col1a2 null line and often not noted until advanced age, therefore the numbers shown above may be an underestimation due to many mice being culled at earlier time points. E-F: Weights of 18 week oim (E) and Col1a2 null (F) mice measured after euthanasia. Blue bars/filled shapes = males, orange bars/open shapes = females. * p-value < 0.05 and *** p-value <0.001. E: p-value for genotype <0.001 for males and females. E-F: n= 13, 11 and 16 for male oim male +/+, +/oim and oim/oim mice respectively, n=13, 12 and 15 for female oim +/+, +/oim and oim/oim mice respectively, n= 21, 17 and 17 for male Col1a2 null +/+, +/-, -/- mice respectively, n=21, 22, 12 for female Col1a2 null +/+, +/-, -/- mice respectively.

Cortical bone analysis and three-point bending of bones from oim and Col1a2 null mice

Cortical thickness was significantly decreased in oim homozygotes; by 33% in 8 week males (Fig. 3A) and to a lesser extent at 18 weeks (22%) (Fig. 3F) and in females (14%; 8 wks, 20%; 18 wks). At 8 weeks cortical thickness in oim heterozygotes was intermediate between that of wild-types and oim homozygotes (a 20% reduction in males and 10% in females). At 18 weeks, but not significantly at 8 or 52 weeks, cortical thickness was also reduced in Col1a2 null homozygotes (18% in males and 10% in females). For oim homozygotes and heterozygotes polar moment of inertia was reduced at 8 weeks (Fig. 3B) in both males (65% and 42% respectively) and females (36% and 26% respectively), and at 18 weeks (Fig. 3G) in males (42% and 29% respectively), indicative of a reduced resistance to torsional loading. In contrast, this parameter was increased by 31% in male 8 week Col1a2 null homozygotes (Fig. 3B) as compared to their control (N +/+) (though not above the level of the oim wild-type control (J +/+)), and at 52 weeks in females by 30% as compared to heterozygotes (Fig. 3L). Periosteal circumference was decreased by 25% and 17% in male oim homozygotes and heterozygotes respectively at 8 weeks (Fig. 3C). However both periosteal (Fig. 3M) and endosteal circumference (Fig. 3N) increased in female Col1a2 null homozygotes at 52 weeks (by 9% and 16%), mirroring the same trend in males. Tissue mineral density was significantly higher in oim wild-types than the other genotypes at 8 weeks (Fig. 3E), but lower in male wild-types at 52 weeks (Fig. 3O).

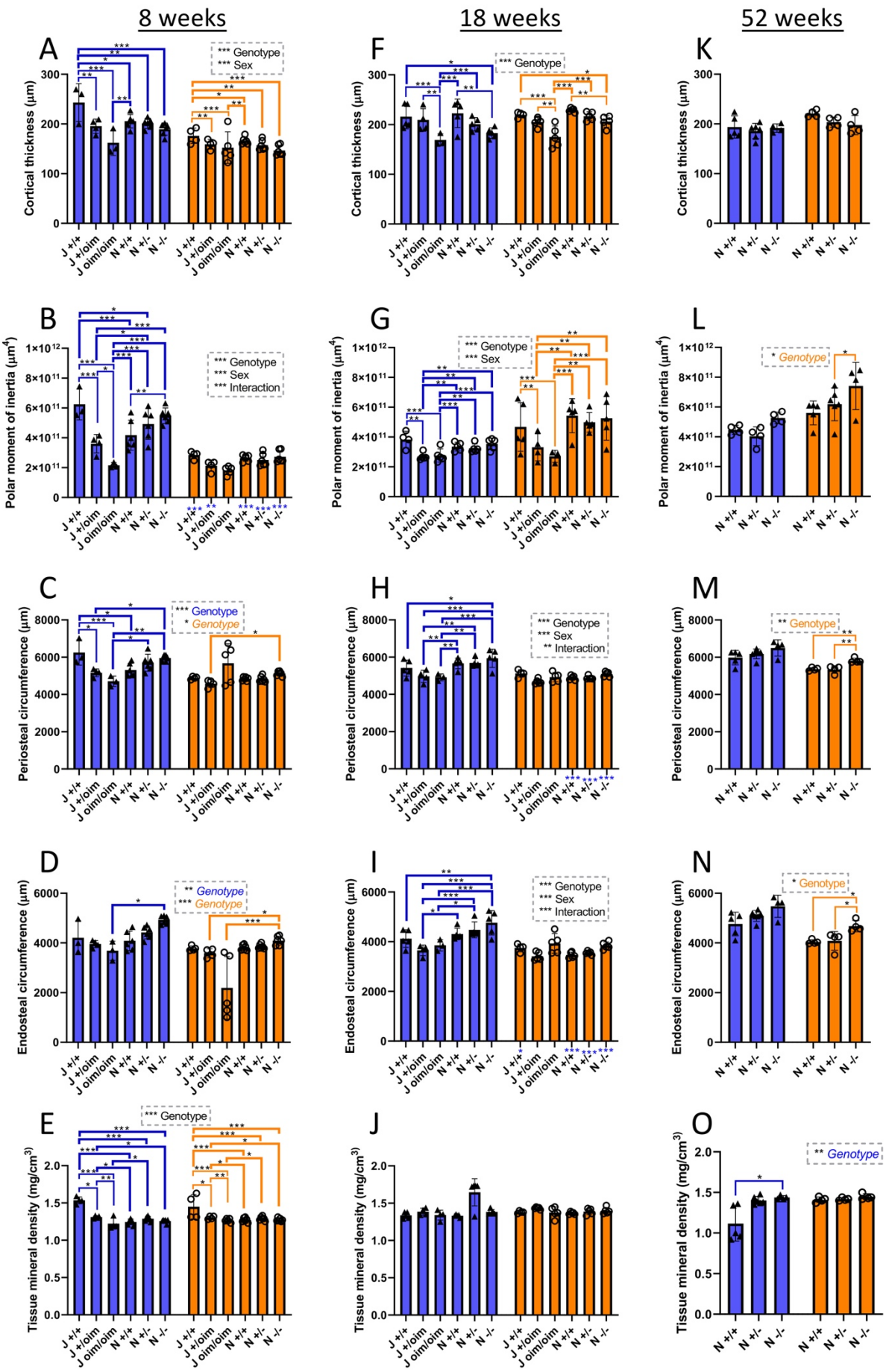
8 weeks
18 weeks
52 weeks
A
B
C
D
E
F
G
H
I
J
K
L
M
N
O
Cortical thickness (µm)
Polar moment of inertia (µm4)
Periosteal circumference (µm)
Endosteal circumference (µm)
Tissue mineral density (mg/cm3)
*** Genotype
*** Sex
*** Interaction
* Genotype
** Genotype
J +/+
J +/oim
J oim/oim
N +/+
N +/-
N -/-

207

Figure 3. Femoral cortical bone analyses of oim and Col1a2 null mice. MicroCT scans were performed on the femur of oim and Col1a2 null mice at 8 (A-E), 18 (F-J) and 52 weeks (K-O). Reconstruction and analysis of scan files enabled determination of cortical thickness (A, F, K), polar moment of inertia (B, G, L), periosteal (C, H, M), and endosteal (D, I, N) circumference, as well as bone density (E, J, O). Blue bars/triangles = males, orange bars/circles = females. Thin blue (male) and orange (female) brackets show differences between genotypes within mouse lines and thick brackets between lines. Male/female differences for particular genotypes are shown below the x-axis for females (blue stars). * p-value < 0.05, ** p-value <0.01 and *** p-value <0.001. N=3 for male oim groups at 8 weeks, except for +/oim and bone density measurements where n=4. N=4 for female oim groups at 8 weeks, except for oim/oim where n=5. N=3 for male oim/oim at 18 weeks, except for bone density where n=4. N=4 for male oim/oim and female +/+, whilst n=5 for other oim groups at 18 weeks. N=6 for all Col1a2 null groups at 8 weeks and n=5 for all Col1a2 null groups at 18 weeks. N=4 for all Col1a2 null groups at 52 weeks, except male +/+ where n=5 and +/- where n=6.

To determine whether biomechanical properties of bones differed between the Col1a2 null and oim lines, femurs and tibias from both male and female mice at various ages were subjected to three-point bending to measure ultimate force, stiffness, stress and elastic modulus (Figs. 4-5). Ultimate force and stiffness were reduced in both male and female oim homozygotes at 8 and 18 weeks in the femur (Fig. 4 A, B, F, G) and the tibia (Fig. 5 A, B, F, G), although differences were not significant in 8 week tibia for which a non-parametric test was used. The cross-sectional area was also reduced at 18 weeks in the femur (by 15% and 22% in males and females respectively) (Fig. 4J), and at 8 weeks (44% in males, 18% in females) and 18 weeks (31% in males, 25% in females) in the tibia (Fig. 5 E, J), consistent with alterations to extrinsic biomechanical properties in oim homozygotes. Ultimate force reductions in the femur were 47% and 65% at 8 and 18 weeks respectively in males, and 51% at both ages in females (Fig. 4 A, F). In the tibia ultimate force was reduced by 54% in males and 44% in females at 18 weeks (Fig. 5F). Stiffness was reduced by 42% and 46% at 8 and 18 weeks in males and by 21% and 42% in females in the femur (Fig. 4B, G), and by 44% and 34% in males and females respectively in the tibia at 18 weeks (Fig. 5G). Only the 8 week femur showed a significantly lower ultimate force for oim heterozygotes (27% for males and 39% for females) (Fig. 4A) whilst stiffness was reduced only in female oim heterozygotes in the tibia at 18 weeks (by 27%) (Fig. 5G). The intrinsic biomechanical property, ultimate stress, was reduced in oim homozygotes in the femur at both 8 (51% in males, 43% in females) and 18 weeks (65% in males, 27% in females) (Fig. 4 C, H), but not in the tibia (Fig 5 C, H). Elastic modulus was unchanged in oim homozygotes in either the femur or tibia (Figs 4&5 D, I).

Deletion of Col1a2 had no effect on 3-point bending parameters in the femur (Fig. 4). In the tibia only ultimate force was reduced (by 35%) in males at 18 weeks of age as compared to the wild-type controls (Fig. 5F), whilst ultimate stress was reduced by 39% as compared to Col1a2 null heterozygotes (Fig. 5H). At 52 weeks only the elastic modulus was affected in males, being reduced by 26% in Col1a2 null homozygotes and 17% in heterozygotes.

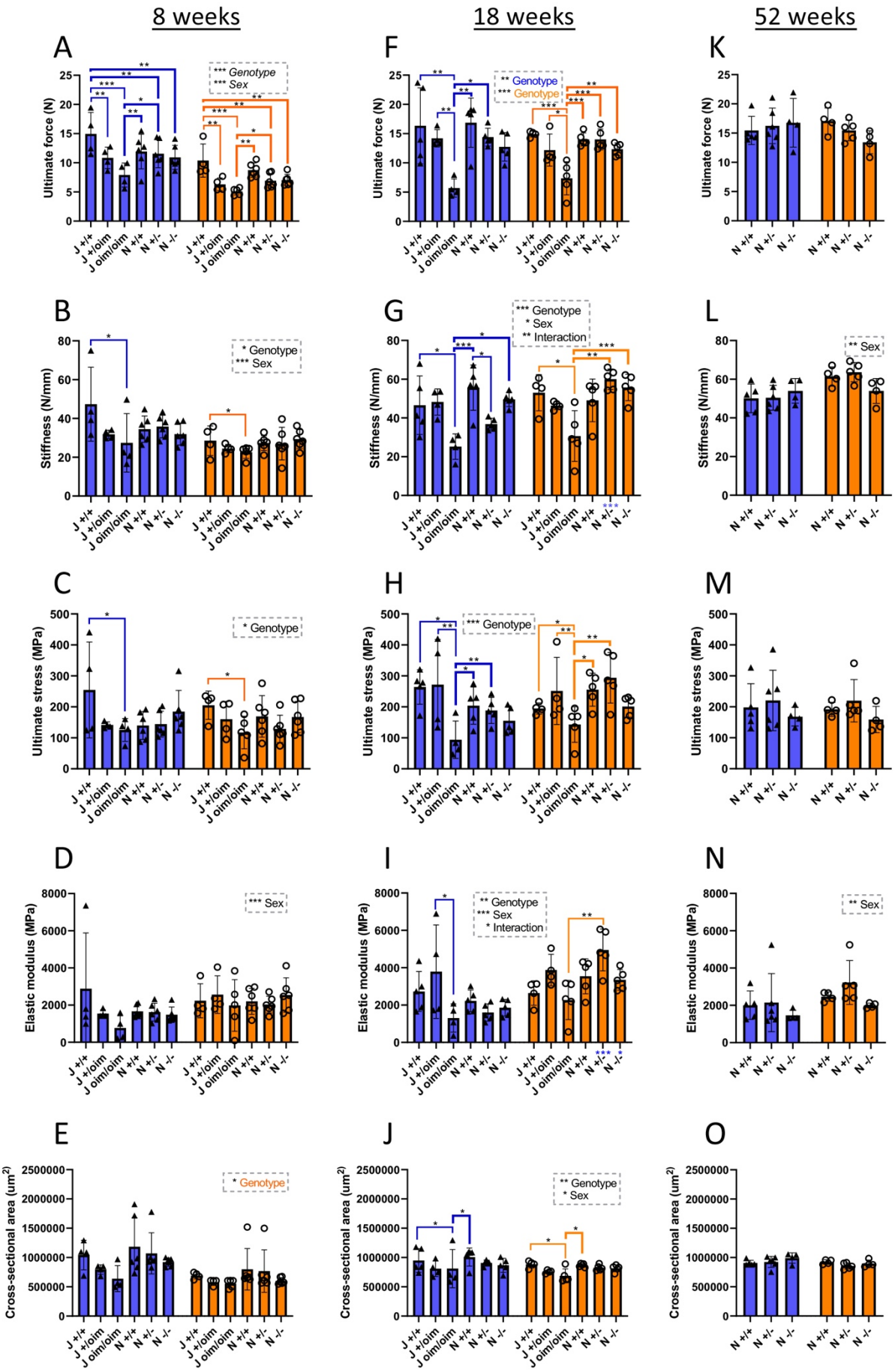
8 weeks
18 weeks
52 weeks
A
B
C
D
E
F
G
H
I
J
K
L
M
N
O
Ultimate force (N)
Stiffness (N/mm)
Ultimate stress (MPa)
Elastic modulus (MPa)
Cross-sectional area (um²)
*** Genotype
*** Sex
** Genotype
*** Genotype
* Genotype
*** Sex
*** Genotype
* Sex
** Interaction
** Sex
* Genotype
*** Genotype
*** Sex
** Genotype
*** Sex
* Interaction
** Sex
* Genotype
** Genotype
* Sex
J +/+
J +/oim
J oim/oim
N +/+
N +/-
N -/-

Figure 4. Three-point bending of femurs from oim and Col1a2 null mice. Femurs from oim and Col1a2 null mice were subjected to three-point bending at 8 (A-E), 18 (F-J) and 52 weeks (K-O). Ultimate force (A, F, K) and stiffness (B, G, L) (extrinsic) measurements were normalised to cross-sectional area (E, J, O) to calculate ultimate stress (C, H, M) and elastic modulus (D, I, N) (intrinsic). Blue bars/triangles = males, orange bars/circles = females. Thin blue (male) and orange (female) brackets show differences between genotypes within mouse lines and thick brackets between lines. Male/female differences for particular genotypes are shown below the x-axis for females (blue stars). * p-value < 0.05, ** p-value <0.01 and *** p-value <0.001. n=4 for all oim groups, except female J oim/oim and male 18 week J+/+ where n=5. n=6 for all Col1a2 null groups at 8 weeks and n=5 for all Col1a2 null groups at 18 weeks. n=4 for all Col1a2 null groups at 52 weeks, except female +/- and male +/+ where n=5 and male +/- where n=6.

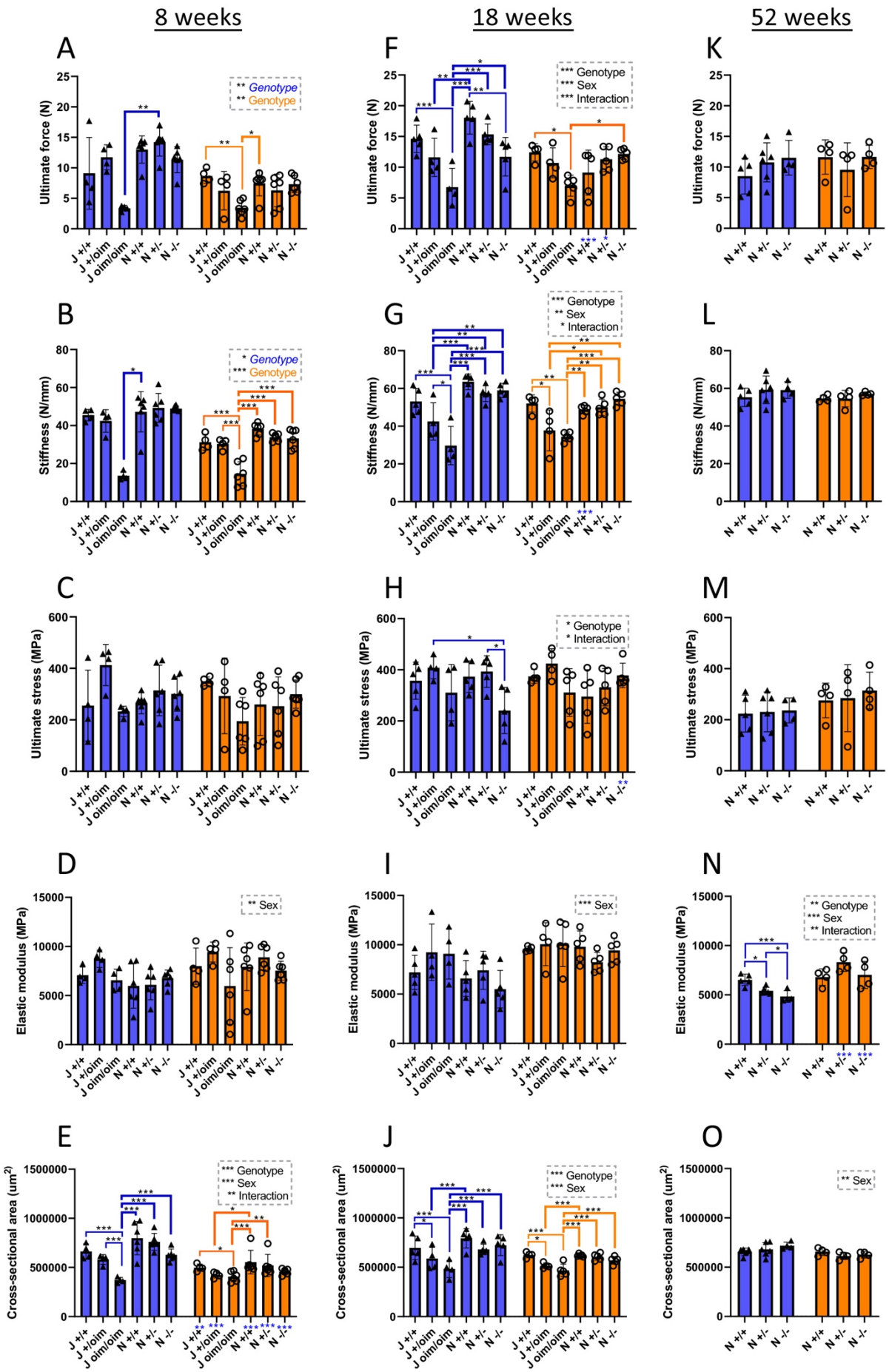
8 weeks
18 weeks
52 weeks
A
B
C
D
E
F
G
H
I
J
K
L
M
N
O
Ultimate force (N)
Stiffness (N/mm)
Ultimate stress (MPa)
Elastic modulus (MPa)
Cross-sectional area (um²)
** Genotype
** Genotype
* Genotype
*** Genotype
*** Genotype
*** Sex
*** Interaction
*** Genotype
** Sex
* Interaction
* Genotype
* Interaction
** Sex
*** Sex
** Genotype
*** Sex
** Interaction
*** Genotype
*** Sex
** Interaction
*** Genotype
*** Sex
** Sex
J +/+
J +/oim
J oim/oim
N +/+
N +/-
N -/-

262

Figure 5. Three-point bending of tibias from oim and Col1a2 null mice. Tibias from oim and Col1a2 null mice were subjected to three-point bending at 8 (A-E), 18 (F-J) and 52 weeks (K-O). Ultimate force (A, F, K) and stiffness (B, G, L) (extrinsic) measurements were normalised to cross-sectional area (E, J, O) to calculate ultimate stress (C, H, M) and elastic modulus (D, I, N) (intrinsic). Blue bars/triangles = males, orange bars/circles = females. Thin blue (male) and orange (female) brackets show differences between genotypes within mouse lines and thick brackets between lines. Male/female differences for particular genotypes are shown below the x-axis for females (blue stars). * p-value < 0.05, ** p-value <0.01 and *** p-value <0.001. n=4 for all oim groups, except female 18 week oim/oim and male 18 week J +/+ where n=5, and female 8 week oim/oim where n=6. n=6 for all Col1a2 null groups at 8 weeks and n=5 for all Col1a2 null groups at 18 weeks. n=4 for all Col1a2 null groups at 52 weeks, except male +/+ where n=5 and male +/- where n=6.

Analysis of trabecular bone of oim and Col1a2 null mice

To analyse differences in trabecular bone structure between genotypes, the proximal tibias from oim and Col1a2 null mice were analysed by µCT (Fig. 6).

There were significant changes in bone volume and architecture in both males and females carrying the oim mutation at both 8 weeks and 18 weeks of age, and most of the differences showed an apparent gene dose effect. In males at 8 weeks, BV/TV was decreased by 42% in heterozygote mice and 80% in homozygous mice compared to wild-type controls (Fig. 6A), due to a decrease in both trabecular thickness (Fig. 6B) and trabecular number (Fig. 6D). The decrease in trabecular thickness and number led to a 151% increase of trabecular separation in oim/oim homozygotes (Fig.6C). Similar changes were observed in female mice at 8 weeks and whilst still pronounced the differences tended to be smaller, and trabecular thickness was unaffected (Fig. 6B). Differences observed for heterozygotes of both sexes were less than those of the respective homozygotes.

At 18 weeks of age, the pattern of the effects of the oim mutation on trabecular bone were similar to those observed at 8 weeks, however the differences between wild-types, heterozygotes and homozygotes were generally smaller. For instance, BV/TV in males was decreased by 50% at 18 weeks (Fig. 6F), compared to 80% at 8 weeks of age (Fig. 6A). There was no longer a significant reduction in trabecular thickness in males, and even an increase in female homozygotes (Fig. 6G).

The only similar alterations resulting from Col1a2 deletion were an 11% decrease in trabecular thickness in 8 week old male null homozygotes and a 10% decrease in heterozygotes (Fig. 6B). Conversely at 52 weeks in males there were Col1a2 loss-dependent increases in BV/TV and trabecular number, with increased connectivity in homozygotes but not heterozygotes. No differences were detected between wild-types of each strain, indicating that this had no influence on the bone structural parameters measured.

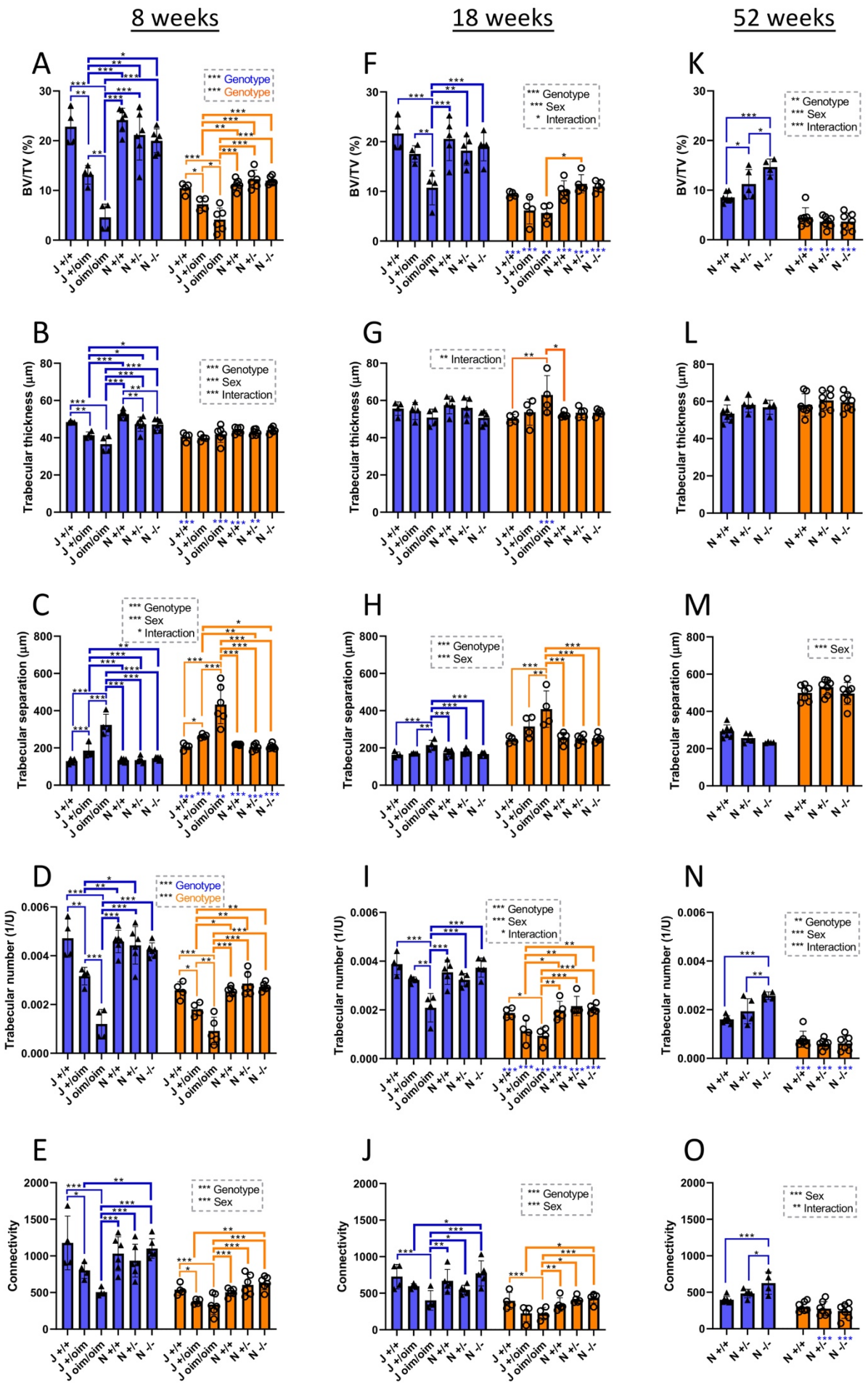
8 weeks
18 weeks
52 weeks
A
B
C
D
E
F
G
H
I
J
K
L
M
N
O
BV/TV (%)
Trabecular thickness (µm)
Trabecular separation (µm)
Trabecular number (1/U)
Connectivity
*** Genotype
*** Sex
* Interaction
** Interaction
** Genotype
J +/+
J +/oim
J oim/oim
N +/+
N +/-
N -/-

Figure 6. Micro-computed tomography bone scans of oim and Col1a2 null mice. MicroCT scans were performed on the knee joints of oim and Col1a2 null mice at 8 (A-E), 18 (F-J) and 52 weeks (K-O). Reconstruction and analysis of scan files enabled determination of bone volume (BV/TV) (A, F, K), trabecular thickness (B, G, L), trabecular separation (C, H, M), trabecular number (D, I, N) and connectivity (E, J, O). Blue bars/triangles = males, orange bars/circles = females. Thin blue (male) and orange (female) brackets show differences between genotypes within mouse lines and thick brackets between lines. Male/female differences for particular genotypes are shown below the x-axis for females (blue stars). * p-value < 0.05, ** p-value <0.01 and *** p-value <0.001. n=4 for all oim groups, except female 8 week old oim/oim where n=6 but n=5 in D. n=6 for all Col1a2 null groups at 8 weeks and n=5 for all Col1a2 null groups at 18 weeks. n=7 for all Col1a2 null groups at 52 weeks, except male +/- where n=5 and male -/- where n=4.

Age-related deterioration of Col1a2 null male homozygotes

The tm1b line (Col1a2 null) was maintained on a mild protocol and mice exceeding the mild severity limit were legally required to be humanely killed. We noted an unexpectedly high loss of male Col1a2 null homozygotes due to a loss of condition, including weight loss and respiratory difficulties. A Kaplan-Meier 'survival' analysis was performed on the Col1a2 null mouse line (Fig. 7). All genotyped mice from this line were included in the analysis up to the age of 12 months, the end point for all experiments. The majority of genotypes had very few losses throughout the time course, with no animals lost for female wild-types and heterozygotes and only one animal lost for female homozygotes, male wild-types and heterozygotes out of a total of 19 mice. In contrast, almost 50% of male homozygotes were lost over the 12 month experimental period.

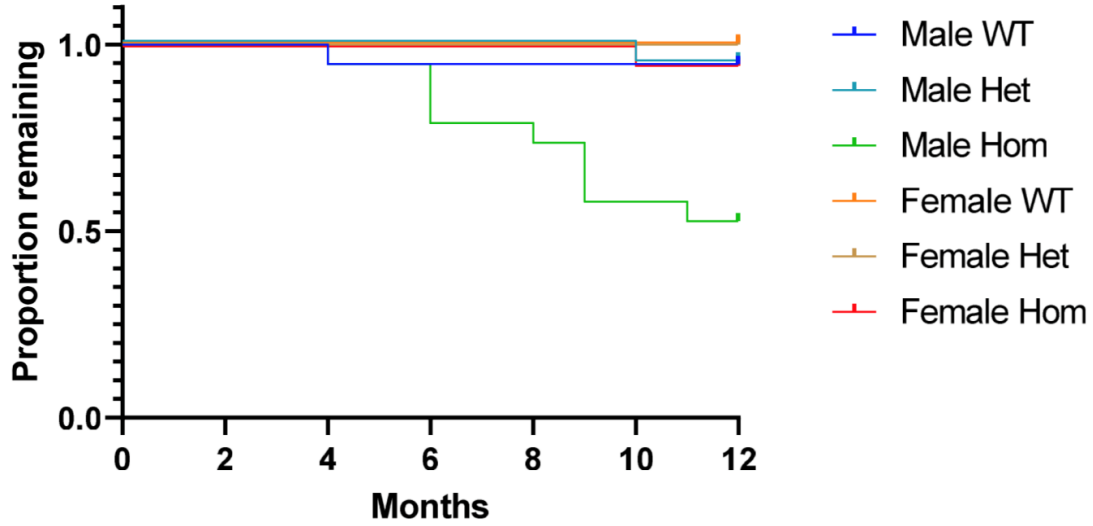

Figure 7. Survival analysis for the Col1a2KO mouse line. A Kaplan-Meier 'survival' analysis was performed on all genotyped mice from the Col1a2 null line up until 12 months (end of experiment). A log-rank (Mantel-Cox) test was performed which gave an overall p-value of <0.0001 indicating a significant difference between survival curves. n=19 for all groups.

Oim heterozygotes do not down-regulate the mutant allele

We considered that the less severe bone phenotype of oim heterozygotes could be related to a compensatory down-regulation of mRNA from the oim mutant allele. A custom allelic discrimination assay indicated that mRNA from both alleles was present in bone tissue from heterozygotes at both 8 (Fig. 8A) and 18 weeks of age (Fig. 8B). Whilst other tissues can be affected in the oim line the bone phenotype is particularly severe. We therefore determined whether there was compensatory downregulation of the mutant allele in tendon at 8 weeks (Fig. 8C) and 18 weeks (Fig. 8D), and in aorta (Fig. 8E), kidney (Fig. 8F), liver (Fig. 8G), or lung (Fig. 8H) at 18 weeks. For all tissues examined, mRNA from both alleles was present at a close to 50-50% ratio in heterozygotes.

Over page:

Figure 8. Allelic discrimination in the oim line. Allelic discrimination was carried out in bone (A-B) and tendon (C-D) at 8 (A, C) and 18 weeks (B, D) and in aorta (E), kidney (F), liver (G) and lung (H) at 18 weeks using ROX labelled primer/probes for the wild-type and VIC for the oim allele channels. For all tissues wild-types displayed little to no VIC signal, whilst homozygotes displayed no ROX signal. Heterozygotes had approximately intermediate signals in both channels with no systematic deviations between sexes or tissues. n=4 for all groups except 8 week bone and tendon samples from male and female oim/oim where n=2-3, 18 week bone and tendon samples from male +/+ where n=5 and female +/oim where n=1, kidney, aorta and lung samples for female +/+ and +/oim where n=3.

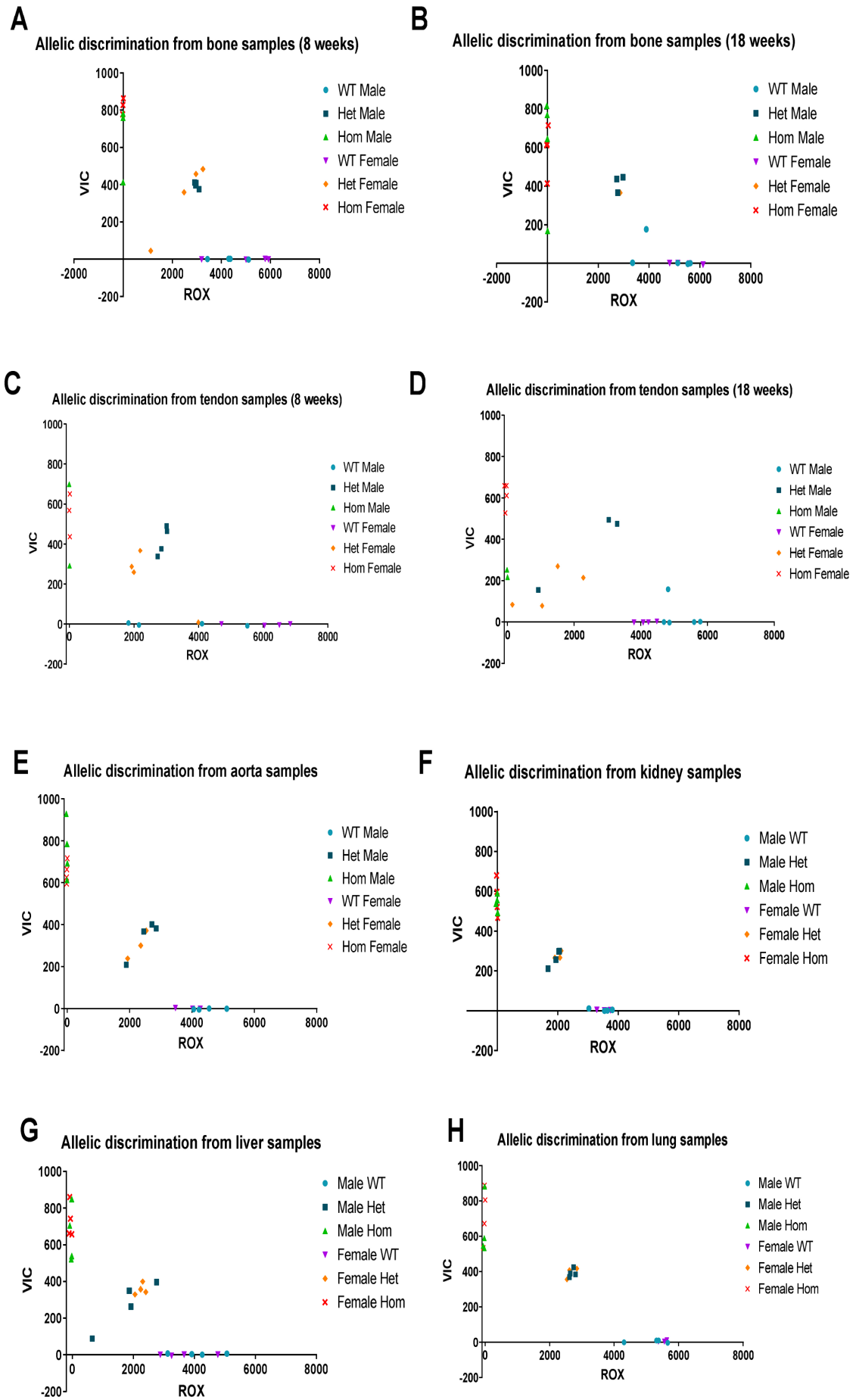

There is a genetic interaction between the oim mutant allele and collagen (I) homotrimer

As the mutant allele is not downregulated in oim heterozygotes, it is feasible that the less severe phenotype relates to gene dosage; given that heterozygotes have 1 rather than 2 copies of the mutant allele. To test this hypothesis we crossed the oim and tm1b lines to produce compound heterozygote offspring, along with heterozygotes of each genotype and wild-type controls (Fig. 9A). Compound heterozygotes contain only one copy of the oim mutant allele but have no wild-type Col1a2 allele so produce solely homotrimeric α1 type I collagen.

The proximal tibias from 8-week-old oim and Col1a2 null (oim/Col1a2 null) cross line mice were analysed by µCT (Fig. 9 B-F). Oim/Col1a2 null compound heterozygotes demonstrated a significantly reduced bone volume (by 49% in males and 21% in females) (Fig. 9B), increased trabecular separation (by 60% in males, 35% in females) (Fig. 9D) and reduced trabecular number (by 40% in males and 24% in females) (Fig. 9E) compared to oim heterozygotes. No significant differences in trabecular thickness (Fig. 9C) and connectivity (Fig. 9F) were detected between compound heterozygotes (-/oim) and oim heterozygotes (+/oim) though differences between Col1a2 null heterozygotes (+/-) and compound heterozygotes were present for connectivity and trabecular thickness, and also between compound heterozygotes and wild-types (+/+) for trabecular thickness. Representative scan images (Fig. 9 G-M) support a structural deterioration with the oim allele as (+/oim) > (-/oim) > (oim/oim), indicating that gene dosage alone does not determine phenotypic severity.

The cortical bone of the femur was also analysed as an indicator of biomechanical properties. Cortical thickness was reduced by 28% in males and 13% in female compound heterozygotes as compared to oim heterozygotes (Fig. S1A). Differences were not detected for other cortical bone parameters (Fig. S1 B-E). Notably in the main 8 week cohort (Fig. 3) differences in cortical bone parameters were only detected between oim heterozygotes and homozygotes for polar moment of inertia in males and for tissue mineral density.

The data for the compound heterozygotes was compared to that of the oim homozygotes and the Col1a2 null line, all of which produce no heterotrimeric type I collagen (Fig. S2). Oim homozygotes and compound heterozygotes demonstrated a reduced bone volume (Fig. S2A) and trabecular thickness (males only) (Fig. S2B), increased trabecular separation (Fig. S2C), and reduced trabecular number (Fig. S2D) and connectivity (Fig. S1E) as compared to Col1a2 null homozygotes. For trabecular parameters, excepting trabecular thickness (Fig. S2B), the bone structural properties of oim homozygotes were inferior to that of compound homozygotes, which were themselves inferior to that of Col1a2 null homozygotes. For example bone volume (Fig. S2A) was reduced by 54% in male and 42% in female compound heterozygotes, but by 77% in male and 67% in female oim homozygotes as compared to Col1a2 null homozygotes. For cortical parameters, cortical thickness was lower in compound heterozygotes than in oim homozygotes or Col1a2 null homozygotes (Fig. S2F), whilst polar moment of inertia (Fig. S2G), periosteal circumference (males only) (Fig. S2H) and endosteal circumference (Fig. S2I) were lower in oim homozygotes and compound heterozygotes than in Col1a2 null homozygotes. Endosteal circumference mirrored the effect on most trabecular parameters with oim homozygotes having inferior bone structural properties than compound heterozygotes, whilst for polar moment of inertia and periosteal circumference (as with trabecular thickness in males) the oim heterozygotes and compound heterozygotes were comparable. Cortical thickness was unusual in that compound heterozygotes had inferior properties to oim homozygotes. Therefore the bone phenotype of the compound heterozygotes was considerably more severe than the Col1a2 null lacking any mutant α2(I) chain, but generally less severe than or similar to the oim homozygotes with two mutant alleles.

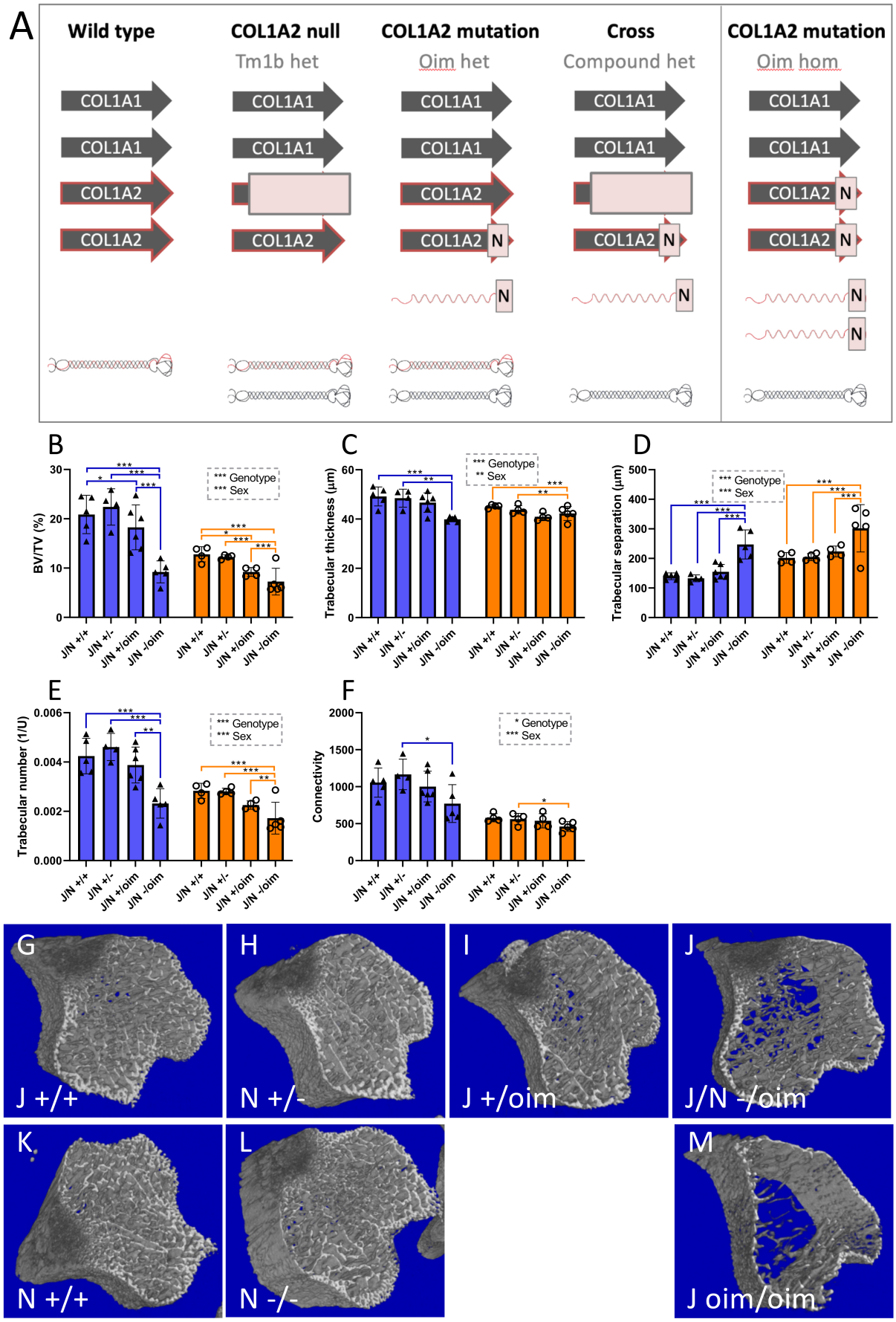
A
Wild type
COL1A2 null
Tm1b het
COL1A2 mutation
Oim het
Cross
Compound het
COL1A2 mutation
Oim hom
COL1A1
COL1A2
N
B
BV/TV (%)
C
Trabecular thickness (µm)
D
Trabecular separation (µm)
E
Trabecular number (1/U)
F
Connectivity
*** Genotype
*** Sex
** Sex
* Genotype
J/N +/+
J/N +/-
J/N +/oim
J/N -/oim
G
J +/+
H
N +/-
I
J +/oim
J
J/N -/oim
K
N +/+
L
N -/-
M
J oim/oim

427
428

429 **Figure 9. Bone structural properties are impaired in compound heterozygotes as compared to**
430 **heterozygotes of the oim or Col1a2 null lines.** A: Genetic differences between the heterozygous oim
431 and Col1a2 null alleles and the compound heterozygous allele, with implications for collagen (I) protein
432 synthesis. The homozygous oim allele is shown for comparison. Arrows indicate COL1 genes; N indicates
433 mutation, light red box indicates null allele. Folded heterotrimeric proteins are indicated in black and
434 red, whilst homotrimers are in black only. The presence of unincorporated mutant Col1a2 allele is
435 indicated as a red waveform with a mutation (N). B-F: MicroCT scans were performed on the knee joints
436 of offspring from heterozygous crosses of each line. Reconstruction and analysis of scan files enabled
437 determination of bone volume (B), trabecular thickness (C), trabecular separation (D), trabecular
438 number (E) and connectivity (F). Blue bars/triangles = males, orange bars/circles = females. Blue and
439 orange brackets show differences between genotypes within males (blue) or females (orange). * p-
440 value < 0.05, ** p-value <0.01 and *** p-value <0.001. n=4 for all groups, except male J/N +/+ and J/N -
441 /oim of both sexes where n=5, and male J/N +/oim where n=6. G-M: Representative scan images from
442 wild-types from the oim line (G), Col1a2 null heterozygotes (H), oim heterozygotes (I), compound
443 heterozygotes (J), wild-types from the Col1a2 null line (K), Col1a2 null homozygotes (L) and oim
444 homozygotes (M). Bone structural defects are more pronounced in compound than in oim
445 heterozygotes.
446
447
448 ## Discussion
449
450 The α2 chain of type I collagen appears largely indispensable to vertebrate life, with heterotrimeric
451 ($(\alpha1)_2(\alpha2)_1$) type I collagen predominating in tetrapods. Actinopterygians (ray-finned fish) even contain
452 a third alpha chain (α3) (42) and there is no obvious homotrimeric ($\alpha1_3$) type I collagen precursor in
453 more distantly related organisms (4, 43). Human and mouse α2(I) chain mutations resulting in
454 homotrimeric type 1 collagen were known to cause brittle bones (18, 25), whilst humans with COL1A2
455 null alleles have cardiac valvular EDS but no overt bone phenotype (32). However common COL1A1
456 alleles resulting in homotrimeric type I collagen are associated with osteoporosis (5). Here we have
457 shown that homotrimeric collagen *per se* largely does not affect bone structural and mechanical
458 properties, but there is pre-weaning loss of male heterozygotes and age-related loss of male null
459 homozygotes as well as a detrimental genetic interaction between the oim mutant Col1a2 allele and
460 the homotrimeric form.
461 To determine the contribution of collagen (I) homotrimer to bone fragility, we compared the
462 bone phenotype of two mouse lines that lack the α2 chain of type I collagen: the oim mutant, a Col1a2
463 null and a combination of the lines. After propagating the lines, we measured a difference in Mendelian
464 inheritance for males from both lines; interestingly this seemed to increase the proportion of wild-type
465 males whilst decreasing the proportion of heterozygotes. To our knowledge pre-weaning loss of male
466 heterozygotes has not been reported for either line. Enzymatic susceptibility assays and differential
467 scanning calorimetry have previously indicated that tail tendon from heterozygous oim mice contains
468 both heterotrimeric and homotrimeric type I collagen (44, 45). Reconstituted fibrils comprising both
469 heterotrimeric and homotrimeric collagen (I) molecules showed subfibrillar segregation of each trimeric
470 form (46). Hence, mixed fibrils in heterozygotes may affect tissue remodelling or mechanics during
471 development resulting in decreased survival of heterozygotes.
472 Unlike oim homozygotes, we observed no fractures in Col1a2 null homozygotes. Bone
473 structural parameters and material properties were largely similar between wild-type, heterozygote
474 and Col1a2 null homozygotes. However, there was a reduction in femoral cortical thickness at 18

weeks, and for males a reduction in ultimate force in the tibia at 18 weeks and trabecular thickness at 8 weeks; paralleling the trend but not the extent of the reduction observed in oim homozygotes. Our results for the oim line at 8 weeks are in agreement with previous studies showing a significant reduction in tibial bone volume and trabecular thickness in oim homozygotes (47) and a significant reduction in ultimate force, stiffness and ultimate stress of the femur (48). By including sex as a factor in our analyses we noted the decrease in tibial trabecular thickness was particular to male homozygotes. Our results for the oim line at 18 weeks were similar to those previously reported for 4 month old mice on the same background although with some differences relating to the significance or gender/sex dependence of the differences (29). In accordance with previous studies, we found no difference in intrinsic elastic modulus or ultimate stress of the tibia of oim homozygotes compared to wild-type controls (29, 48, 49), although ultimate stress but not elastic modulus was decreased in the femur. Decreased femoral ultimate stress was previously reported for 12-14 week oim homozygotes (50, 51), but not in all studies (52). Oim homozygote mice were lighter and visually smaller than their wild-type and heterozygote littermates, therefore the differences seen in extrinsic but not intrinsic mechanical properties, particularly of the tibia, between oim homozygotes and wild-types could imply that the increased bone fragility of oim homozygotes is due to the reduced size of these mice. Cross-sectional area was significantly reduced in the tibia at both ages, and in the femur at 18 weeks, though not at 8 weeks. microCT analysis however indicates some intrinsic differences in bone structure, with reduced cortical and trabecular bone.

Col1a2 null homozygotes did not display bone fragility but swollen joints were identified in males who also displayed age-related deterioration in condition. Human COL1A2 null homozygotes have cardiac valvular Ehlers-Danlos syndrome (cvEDS) (32, 33) hence the age-related deterioration in mice may relate to cardiovascular abnormalities. Indeed the International Mouse Phenotyping Consortium reports dilated left heart ventricle in males measured at 12 weeks of age and increased heart weight at 16 weeks in Col1a2 null homozygotes (53). Cardiovascular abnormalities were however observed in mice of both sexes and cvEDS patients are not solely male. It may be that cardiovascular defects present earlier in male mice due to increased activity or remain subclinical in females. IMPC also reported a skeletal phenotype for Col1a2 null male mice with increased (notably not decreased) bone mineral content and density (DEXA, 14 weeks) and “abnormal” femur and tibia morphology (X-ray, 14 weeks). Reported phenotypes change over time due to continual addition of control samples, but alterations to body fat in males and increased circulating alkaline phosphates in females were also listed. In the present study, loss of Col1a2 appeared to improve some bone structural parameters by 52 weeks (periosteal and endosteal circumference in females, tissue mineral density, trabecular bone volume, trabecular number and connectivity in males), possibly reflecting lower turnover of homotrimeric collagen (I). Elastic modulus was however reduced in Col1a2 null males by 52 weeks indicative of some altered bone material properties. Overall a combination of early loss of heterozygous males and age-related deterioration in null homozygotes could exert selective pressure to maintain the heterotrimeric form of type I collagen in vertebrate populations.

Whilst the strain of the lines differs slightly (C57BL/6J versus C57BL/6N), similar cortical and trabecular bone parameters have been reported in both strains (54). In the present study, differences were detected between wild-types of each strain at 8 weeks for cortical thickness (Fig. 3A) and tissue mineral density (Fig. 3E) in both sexes, and for polar moment of inertia (Fig. 3B) and periosteal circumference (Fig. 3C) in males. However for cortical thickness and polar moment of inertia the oim homozygotes (J oim/oim) were still significantly lower than the Col1a2 wild-types (N +/+) as well as than wild-types of their background strain (J +/+). For 3-point bending parameters of either the femur or tibia there were no significant differences between wild-types of either strain. Hence solely periosteal

521 circumference and tissue mineral density differences may be influenced by the background strain.
522 Reduced periosteal circumference in male compound heterozygotes (but not cortical thickness, polar
523 moment of inertia or endosteal circumference) could therefore be influenced by the mixed 6J/6N
524 background.
525 A key finding of this study was that the bone phenotype of a single copy of the oim allele was
526 exacerbated by the absence of heterotrimeric type I collagen; i.e. that oim heterozygotes had a less
527 severe phenotype than compound oim/null heterozygotes. Notably the phenotype of oim homozygotes
528 still appeared more severe than that of compound heterozygotes, indicating some gene dosage effect
529 for the mutant allele. Oim heterozygotes do not down-regulate the mutant allele (Fig. 7) hence
530 presumably there is no mechanism to detect the oim mutation prior to translation or trimerization.
531 Despite the severe bone phenotype in oim homozygotes, and whilst ER stress has been demonstrated
532 in other OI models (37-41) we detected no evidence of increased ER stress by qPCR or by osteoblast
533 ultrastructural analysis (not shown). A report indicating that relieving ER stress improves femoral
534 mechanical properties in oim heterozygotes, actually demonstrated no difference between placebo and
535 treatment groups and did not monitor ER stress (55). We did observe several significant differences
536 between oim heterozygotes and wild-type controls, including all tibial structural parameters and
537 femoral ultimate force at 8 weeks. At 18 weeks differences were limited to tibial stiffness in females
538 and tibial cross-sectional area, consistent with a previous study which reported few significant
539 differences between wild-types and heterozygotes at 18 weeks (Yao et al., 2013). Hence bone structural
540 parameters can improve between 8 and 18 weeks in both heterozygotes and homozygotes. In oim
541 heterozygotes at 8 weeks it is unclear if the observed differences in bone parameters relate solely to
542 the interaction between the oim mutant allele and the proportion of homotrimeric collagen (I) that was
543 present, or if the oim allele alone exerts an effect. The genetic interaction between the oim allele and
544 homotrimeric collagen (I) could relate to the process of collagen folding and trimerization within the
545 endoplasmic reticulum. The observed allelic series is consistent with a model in which the abnormal
546 alpha-2 chain trimerises with two normal alpha-1 chains, but results in trimer degradation and
547 concurrent suppression of collagen fibril assembly. Alternatively the homotrimeric collagen (I) could
548 alter cell-matrix interactions to modulate cellular stress responses, if present. Procollagen N- and C-
549 propeptides, derived from the proteolytic cleavage of procollagen, have been shown to have
550 intracellular roles in modulating protein synthesis (56-58) whilst homotrimeric triple helical regions
551 increased proliferation and migration as compared to heterotrimeric pepsinised collagen (11). Hence
552 homotrimeric forms of collagen fibrils or propeptides have the potential for altered signalling affecting
553 cellular stress responses. The association of homotrimeric type I collagen with several common human
554 age-related diseases, in which it is unlikely to predominate structurally, could therefore relate to
555 altered cellular signalling or cell stress responses.
556 The experiments outlined above demonstrate a genetic interaction between homotrimeric
557 collagen (I) and the oim mutant allele, suggesting that the presence of heterotrimeric collagen (I) in oim
558 heterozygotes alleviates the effect of the oim mutant allele in bone.
559
560
561 ## Materials and Methods
562
563 **Mouse models**
564 A Col1a2 knock-out mouse line (Col1a2$^{tm1b(EUCOMM)Wtsi}$, C57BL/6N) (Col1a2 null, N) and osteogenesis
565 imperfecta mouse line (Col1a2^{oim}, C57BL/6J) (oim, J) were used to investigate the effects of the absence
566 and the mis-folding of the α2(I) polypeptide chain respectively (Fig. 1B). The Col1a2$^{tm1b(EUCOMM)Wtsi}$ line

567 was derived from Col1a2$^{tm1a(EUCOMM)Wtsi}$, purchased from the Mutant Mouse Resource and Research
568 Centre (MMRRC) at UC Davies, by Cre-mediated recombination (59) during IVF provided by MRC
569 Harwell. The Col1a2^{oim} line was a kind gift from Prof. Charlotte Phillips, University of Missouri and was
570 subsequently rederived using Charles River (Massachusetts, USA) services. The strains have been
571 deposited and are available from the MMRRC (RRID 66964, C57BL/6N-
572 Col1a2<tm1b(EUCOMM)Wtsi>/LaelMmnc and RRID 66518, B6J.Cg-*Col1a2^{oim}*/McbrMmnc). Mice were
573 housed at the University of Liverpool in a specific pathogen free unit in groups of up to 5 by litter, with
574 oim homozygotes and Col1a2 null/oim heterozygotes housed separately after weaning. Food and water
575 were supplied *ad libitum* and wet food was supplied to oim homozygotes and Col1a2 null/oim
576 heterozygotes due to fragile teeth. Cage balconies were removed for oim homozygotes and Col1a2
577 null/oim heterozygotes to reduce fracture risk and non-tangling bedding was supplied as standard for
578 all mice. The mice were housed in the same room at 20-24°C and 45-65% humidity with a 12 hour
579 light/dark cycle. All breeding and maintenance of animals was performed under project licences
580 PP4874760 and P92F55CB2, in compliance with the Animals (Scientific Procedures) Act 1986 and UK
581 Home Office guidelines. Details of all animals were recorded on tick@lab (a-tune) laboratory animal
582 management software (Darmstadt, Germany), including health and treatment reports. Genotyping was
583 carried out using Transnetyx (Tennessee, USA) services using the 'Col1a2-2 WT' probe with 'LAC Z' or
584 'L1L2-Bact-P TA' for tm1a allele or 'L1L2 tm1b' for tm1b allele, and the 'oim' probe for the oim line.
585 Blinding was carried out by processing mice and labelling samples according to the mouse number,
586 rather than genotype, however KJL was responsible for the initial allocation of animals to specific
587 experimental groups. Wild-type (N +/+, J +/+), heterozygote (N +/-, J +/oim) and homozygote (N -/-, J
588 oim/oim) mice were sacrificed at 8 (±3 days) and 18 (±3 days) weeks for analysis as well as 52 weeks (±8
589 days) for the Col1a2 null line. Eight and 18 weeks were chosen as the time points at which long bone
590 growth and bone mineralisation respectively are complete. Oim mice were not maintained up to 52
591 weeks due to welfare considerations for homozygotes exhibiting spontaneous fractures. Cross-breeding
592 of both lines was also performed (Col1a2 null/oim, mixed background) and wild-type (+/+), Col1a2 null
593 heterozygote (+/oim), oim heterozygote (+/-) and compound heterozygote (-/oim) mice were sacrificed
594 at 8 weeks. A total of 281 mice were used in this study, excluding those from which solely 'survival' and
595 health analyses were derived. No mice were excluded from experimental groups.
596
597 **Mouse dissection**
598 Mice were culled using a rising carbon dioxide concentration method in an automated CO_2 delivery
599 chamber. After confirmation of the permanent cessation of the circulation, the mice were weighed and
600 the tail was removed at the base and added to PBS for further dissection. Next, the skin was removed,
601 the femoral heads displaced from the acetabulum and the entire hind limbs detached and added to
602 PBS. The skin was then removed from the tail and the tail tendons dissected free. Excess muscle was
603 removed from the hind limbs and the feet removed at the tarsus. For techniques requiring isolated
604 tendon and bone tissue, the patellar tendon was further removed, the femur and tibia separated, and
605 all muscle dissected out.
606
607 **Pulse-chase with ^{14}C-L-proline**
608 Tail tendon, patellar tendon and femur tissue was dissected from 8 week old Tm1b mice. Tissue was
609 dissected into small pieces and added to DMEM containing penicillin/streptomycin (1% v/v), L-
610 glutamine (2 mM), L-ascorbic acid 2-phosphate (200 µM), β-aminopropionitrile (400 µM) and 2.5 µCi/ml
611 [^{14}C]proline (GE Healthcare, Illinois, USA) and incubated at 37°C for 18 hours. The tissue samples were
612 subsequently moved to media without [^{14}C]proline for 3 hours. Collagen was then extracted from the

613 tissue samples using a salt extraction buffer (1 M NaCl, 25 mM EDTA, 50 mM Tris-HCl, pH 7.4)
614 containing protease inhibitors (Roche, Basel, Switzerland). Samples were extracted overnight at 4°C
615 with agitation. Extracts were analysed by electrophoresis on 6% Tris-Glycine gels (ThermoFisher,
616 Massachusetts, USA) with delayed reduction (60). The gels were fixed (10% methanol, 10% acetic acid),
617 dried under vacuum, and exposed to a phosphorimaging plate (BAS-IP MS). Phosphorimaging plates
618 were processed using a phosphorimager (Typhoon FLA7000 IP) and densitometry carried out using
619 ImageQuant software (GE Healthcare Life Sciences, Illinois, USA).
620
621 **Three point bending**
622 Before three-point bending tests, the freshly isolated intact femurs and tibias (only those showing no
623 evidence of fracture calluses) were imaged using uCT in order to obtain the cross-sectional area,
624 circumference and moment of inertia measurements. Bones were scanned inside 1 ml syringes in PBS
625 using a Skyscan 1272 scanner (Bruker, Kontich, Belgium). Scans were performed at a resolution of 9 µm
626 (60 kV, 150 µA, 2x2 binning, rotation step size 0.5°, using a 0.5 mm aluminium filter). Scans were
627 reconstructed using NRecon (Bruker, Kontich, Belgium) using Gaussian smoothing of 1, ring artefact
628 reduction 5, and beam hardening compensation at 38%. For analysis of cortical bone parameters, a
629 region of interest of 200 slices of the mid-femur and mid-tibia was selected and saved using Dataviewer
630 (Bruker, Kontich, Belgium). Cross-sectional area for both bones, then cortical thickness, bone perimeter,
631 periosteal circumference, second moment of area about the mediolateral axis and polar moment of
632 inertia as well as bone density measurements for the femur, were obtained using custom macros in
633 CTan (Bruker, Kontich, Belgium). Endosteal circumference was calculated using equation 1.1. Density
634 measurements were calibrated using a set of hydroxyapatite phantoms (Bruker, Kontich, Belgium).
635
636 **Eq. 1.1**
637 Endosteal circumference = bone perimeter – periosteal circumference
638
639 A Zwickiline Fmax 1 kN (Zwick, Ulm, Germany) biomechanical tester fitted with a 50N load cell
640 was used for three-point bending experiments. Femurs and tibias were loaded at a span length of 8 mm
641 and the crosshead was lowered at a rate of 0.5 mm/min using testXpert II software (Zwick). Ultimate
642 force and stiffness measurements were calculated from the force-displacement curve, at the point of
643 maximum load and the maximum gradient of the linear rising section of the graph respectively. The
644 maximum stiffness and elastic modulus. were calculated as described (61)
645
646 **Micro computed tomography (uCT)**
647 Hind limbs were fixed overnight in 10% neutral buffered formalin before washing and storage in 70%
648 ethanol. Limbs were loaded into 2 ml syringe tubes in 70% ethanol and scanned using a Skyscan 1272
649 scanner (Bruker, Kontich, Belgium) at a resolution of 4.5 µm(60 kV, 150 µA, no binning, rotation step
650 size 0.3°, using a 0.5 mm aluminium filter). Scans were reconstructed using NRecon software (Bruker) as
651 described above. Trabecular bone parameters of the proximal tibia were measured in a volume,
652 selected and saved using Dataviewer (Bruker), of 200 slices starting 20 slices distal to the growth plate
653 as described (62). As previously, only bones that did not contain any fracture calluses were used.
654 Trabecular bone parameters were measured using a custom macro in CTan (Bruker).
655
656 **Allelic discrimination**
657 RNA was extracted from tissues preserved in RNAlater by firstly applying Trizol to samples which were
658 then homogenised using a steel ball lysing matrix and a FastPrep 24 tissue homogeniser (MP Biomedicals,

California, USA). RNA was extracted from homogenised samples using a Direct-Zol RNA kit (Zymo Research, California, USA) as per the manufacturer's instructions. The quantity and quality of RNA was assessed using a NanoDrop spectrophotometer (Thermo Fisher, Massachusetts, USA), 260/280 values between 1.8-2.1 were deemed of a sufficient RNA quality. cDNA was synthesised in a 25 µl reaction from 0.5-1 µg of total RNA. The conditions for cDNA synthesis were: incubation at 5 minutes at 70°C, 60 minutes at 37°C and 5 minutes at 93°C with 1 U/µl RNasin ribonuclease inhibitor, 2 mM PCR nucleotide mix, 8 U/µl M-MLV reverse transcriptase and 0.02 µg/µl random-hexamer oligonucleotides per reaction.

Detection of murine Col1a2 wild-type and mutant alleles was performed using a custom snpsig™ real-time PCR mutation detection/allelic discrimination kit (Primerdesign, Southampton, UK). 10 ng of cDNA was added to 10 µl of PrecisionPLUS mastermix (Primerdesign, Southampton, UK), 1 µl of the custom genotyping primer/probe mix and 4 µl nuclease free water per reaction. Amplification was performed on a Stratagene qPCR machine with an initial enzyme activation step of 2 minutes at 95°C followed by 10 cycles of denaturation for 10 seconds at 95°C and extension for 60 seconds at 60°C. Finally, 35 cycles of denaturation for 10 seconds at 95°C and extension for 60 seconds at 68°C, with fluorogenic data collected during this extension step for the ROX (wild type) and VIC (oim) channels.

Statistical analysis

Sample size calculations were carried out using G*Power 3.1.9.2 and Stata13 to give a power of at least 90% at the 5% level of significance. Primary outcomes were defined as bone stiffness (N/mm), bone volume (%) and trabecular separation (µm) with a standardised effect size of 2 deemed to be biologically important. For comparison, effect sizes were calculated from previously reported oim data (48) as -2.0 (41%) for femur stiffness, -2.8 (48%) for bone volume and 2.8 (66%) for trabecular separation. Comparison of 'bone mineral density' (DEXA) effect sizes for the oim (63) and Col1a2 null lines (53) at 14 wks indicated effect sizes of a similar magnitude (d=-1.6 and 1.7 respectively). Group sizes of 3 were calculated for two-way ANOVA on normally distributed data to test the effect of genotype (Stata13). The sample size in each group was increased by 20% to allow for non-normality of the data to give planned group sizes of 4.

All statistical analysis was completed using SigmaPlot 14.0 or 14.5 software. Comparisons of continuous measurements across sex and genotype were carried out using a two-way ANOVA with a Holm-Sidak post-hoc test. Where residuals did not meet assumptions of normality (Shapiro-Wilk test) or equal variance (Brown-Forsythe test), data were transformed with a Box-Cox or Johnson transformation using Mintab 18 before analysis. If a suitable transformation was not identified, male and female datasets were analysed separately using a one-way ANOVA (denoted with coloured font on graphs). If residuals still did not meet assumptions a nonparametric Kruskal-Wallis one-way ANOVA on ranks with a Dunn's post-hoc test was used for comparisons (italicised on graphs). Comparisons of two categorical variables were done via a chi-squared test with the expected counts in each cell of the table being at least 5. The time to deterioration data were summarised via survival curves and statistically compared via a log-rank (Mantel-Cox) test, overall p-value is reported. No data points were excluded from statistical analysis. Data were plotted using GraphPad Prism 8.

Author Contributions

KJL: Data curation, Formal Analysis, Investigation, Project administration, Supervision, Visualization, Writing – original draft, Writing – review & editing; LR: Data curation, Investigation, Visualization; GBG: Funding acquisition, Methodology, Writing – review & editing; PC: Conceptualization, Funding acquisition, Writing – review & editing; RA: Funding acquisition, Methodology, Writing – review &

editing; GC: Formal Analysis, Funding acquisition, Writing – review & editing; RVH: Data curation, Investigation, Funding acquisition, Investigation, Methodology, Software, Supervision, Visualization, Writing – review & editing; EGC-L: Conceptualization, Formal Analysis, Funding acquisition, Project administration, Supervision, Visualization, Writing – original draft, Writing – review & editing.

Acknowledgements

The study was funded by the UK Medical Research Council (MR/R00319X/1). LR was supported by the Erasmus+ program.

References

1. Canty EG, Kadler KE. Procollagen trafficking, processing and fibrillogenesis. J Cell Sci. 2005;118(Pt 7):1341-53.
2. Lees JF, Tasab M, Bulleid NJ. Identification of the molecular recognition sequence which determines the type-specific assembly of procollagen. EMBO J. 1997;16(5):908-16.
3. Sharma U, Carrique L, Vadon-Le Goff S, Mariano N, Georges RN, Delolme F, et al. Structural basis of homo- and heterotrimerization of collagen I. Nat Commun. 2017;8:14671.
4. DiChiara AS, Li RC, Suen PH, Hosseini AS, Taylor RJ, Weickhardt AF, et al. A cysteine-based molecular code informs collagen C-propeptide assembly. Nat Commun. 2018;9(1):4206.
5. Ralston SH, Uitterlinden AG, Brandi ML, Balcells S, Langdahl BL, Lips P, et al. Large-scale evidence for the effect of the COLIA1 Sp1 polymorphism on osteoporosis outcomes: the GENOMOS study. PLoS Med. 2006;3(4):e90.
6. Philp AM, Collier RL, Grover LM, Davis ET, Jones SW. Resistin promotes the abnormal Type I collagen phenotype of subchondral bone in obese patients with end stage hip osteoarthritis. Scientific reports. 2017;7(1):4042.
7. Kerns JG, Gikas PD, Buckley K, Shepperd A, Birch HL, McCarthy I, et al. Evidence from Raman Spectroscopy of a Putative Link Between Inherent Bone Matrix Chemistry and Degenerative Joint Disease. Arthritis & Rheumatology. 2014;66(5):1237-46.
8. Bailey AJ, Sims TJ, Knott L. Phenotypic expression of osteoblast collagen in osteoarthritic bone: production of type I homotrimer. Int J Biochem Cell Biol. 2002;34(2):176-82.
9. Zhong B, Huang D, Ma K, Deng X, Shi D, Wu F, et al. Association of COL1A1 rs1800012 polymorphism with musculoskeletal degenerative diseases: a meta-analysis. Oncotarget. 2017;8(43):75488-99.
10. Brull DJ, Murray LJ, Boreham CA, Ralston SH, Montgomery HE, Gallagher AM, et al. Effect of a COL1A1 Sp1 binding site polymorphism on arterial pulse wave velocity: an index of compliance. Hypertension. 2001;38(3):444-8.
11. Makareeva E, Han S, Vera JC, Sackett DL, Holmbeck K, Phillips CL, et al. Carcinomas Contain a Matrix Metalloproteinase–Resistant Isoform of Type I Collagen Exerting Selective Support to Invasion. Cancer Res. 2010;70(11):4366-74.
12. Rojkind M, Giambrone MA, Biempica L. Collagen Types in Normal and Cirrhotic Liver. Gastroenterol. 1979;76(4):710-9.
13. Ehrlich HP, Brown H, White BS. Evidence for type V and I trimer collagens in Dupuytren's Contracture palmar fascia. Biochem Med. 1982;28(3):273-84.
14. Han S, Makareeva E, Kuznetsova NV, DeRidder AM, Sutter MB, Losert W, et al. Molecular mechanism of type I collagen homotrimer resistance to mammalian collagenases. J Biol Chem. 2010;285(29):22276-81.

754 15. Sims TJ, Miles CA, Bailey AJ, Camacho NP. Properties of collagen in OIM mouse tissues. Connect
755 Tissue Res. 2003;44 Suppl 1:202-5.
756 16. Pfeiffer BJ, Franklin CL, Hsieh FH, Bank RA, Phillips CL. Alpha 2(I) collagen deficient oim mice
757 have altered biomechanical integrity, collagen content, and collagen crosslinking of their thoracic aorta.
758 Matrix Biol. 2005;24(7):451-8.
759 17. Carriero A, Zimmermann EA, Paluszny A, Tang SY, Bale H, Busse B, et al. How tough is brittle
760 bone? Investigating osteogenesis imperfecta in mouse bone. J Bone Miner Res. 2014;29(6):1392-401.
761 18. Chipman SD, Sweet HO, McBride DJ, Jr., Davisson MT, Marks SC, Jr., Shuldiner AR, et al.
762 Defective pro alpha 2(I) collagen synthesis in a recessive mutation in mice: a model of human
763 osteogenesis imperfecta. PNAS. 1993;90(5):1701-5.
764 19. Carleton SM, McBride DJ, Carson WL, Huntington CE, Twenter KL, Rolwes KM, et al. Role of
765 genetic background in determining phenotypic severity throughout postnatal development and at peak
766 bone mass in Col1a2 deficient mice (oim). Bone. 2008;42(4):681-94.
767 20. Grabner B, Landis WJ, Roschger P, Rinnerthaler S, Peterlik H, Klaushofer K, et al. Age- and
768 genotype-dependence of bone material properties in the osteogenesis imperfecta murine model (oim).
769 Bone. 2001;29(5):453-7.
770 21. Vouyouka AG, Pfeiffer BJ, Liem TK, Taylor TA, Mudaliar J, Phillips CL. The role of type I collagen
771 in aortic wall strength with a homotrimeric. J Vasc Surg. 2001;33(6):1263-70.
772 22. Misof K, Landis WJ, Klaushofer K, Fratzl P. Collagen from the osteogenesis imperfecta mouse
773 model (oim) shows reduced resistance against tensile stress. J Clin Invest. 1997;100(1):40-5.
774 23. Phillips CL, Pfeiffer BJ, Luger AM, Franklin CL. Novel collagen glomerulopathy in a homotrimeric
775 type I collagen mouse (oim). Kidney Int. 2002;62(2):383-91.
776 24. Nicholls AC, Pope FM, Schloon H. Biochemical heterogeneity of osteogenesis imperfecta: New
777 variant. Lancet. 1979;1(8127):1193.
778 25. Nicholls AC, Osse G, Schloon HG, Lenard HG, Deak S, Myers JC, et al. The clinical features of
779 homozygous alpha 2(I) collagen deficient osteogenesis imperfecta. J Med Genet. 1984;21(4):257-62.
780 26. Pace JM, Wiese M, Drenguis AS, Kuznetsova N, Leikin S, Schwarze U, et al. Defective C-
781 propeptides of the proalpha2(I) chain of type I procollagen impede molecular assembly and result in
782 osteogenesis imperfecta. J Biol Chem. 2008;283(23):16061-7.
783 27. Saban J, Zussman MA, Havey R, Patwardhan AG, Schneider GB, King D. Heterozygous oim mice
784 exhibit a mild form of osteogenesis imperfecta. Bone. 1996;19(6):575-9.
785 28. Camacho NP, Hou L, Toledano TR, Ilg WA, Brayton CF, Raggio CL, et al. The material basis for
786 reduced mechanical properties in oim mice bones. J Bone Miner Res. 1999;14(2):264-72.
787 29. Yao X, Carleton SM, Kettle AD, Melander J, Phillips CL, Wang Y. Gender-dependence of bone
788 structure and properties in adult osteogenesis imperfecta murine model. Ann Biomed Eng.
789 2013;41(6):1139-49.
790 30. Prockop DJ. Osteogenesis imperfecta. A model for genetic causes of osteoporosis and perhaps
791 several other common diseases of connective tissue. Arthritis Rheum. 1988;31(1):1-8.
792 31. Mann V, Hobson EE, Li B, Stewart TL, Grant SFA, Robins SP, et al. A COL1A1 Sp1 binding site
793 polymorphism predisposes to osteoporotic fracture by affecting bone density and quality. J Clin Invest
794 2001;107(7):899-907.
795 32. Malfait F, Symoens S, Coucke P, Nunes L, De Almeida S, De Paepe A. Total absence of the
796 alpha2(I) chain of collagen type I causes a rare form of Ehlers-Danlos syndrome with hypermobility and
797 propensity to cardiac valvular problems. J Med Genet. 2006;43(7):e36.
798 33. Guarnieri V, Morlino S, Di Stolfo G, Mastroianno S, Mazza T, Castori M. Cardiac valvular Ehlers-
799 Danlos syndrome is a well-defined condition due to recessive null variants in COL1A2. Am J Med Genet
800 A. 2019;179(5):846-51.
801 34. Maruelli S, Besio R, Rousseau J, Garibaldi N, Amiaud J, Brulin B, et al. Osteoblasts mineralization
802 and collagen matrix are conserved upon specific Col1a2 silencing. Matrix Biol Plus. 2020;6-7:100028.
803 35. Makareeva E, Aviles NA, Leikin S. Chaperoning osteogenesis: new protein-folding disease
804 paradigms. Trends Cell Biol. 2011;21(3):168-76.
805 36. Forlino A, Cabral WA, Barnes AM, Marini JC. New perspectives on osteogenesis imperfecta. Nat
806 Rev Endocrinol. 2011;7(9):540-57.

807 37. Chessler SD, Byers PH. BiP binds type I procollagen pro alpha chains with mutations in the
808 carboxyl-terminal propeptide synthesized by cells from patients with osteogenesis imperfecta. J Biol
809 Chem. 1993;268(24):18226-33.
810 38. Lisse TS, Thiele F, Fuchs H, Hans W, Przemeck GK, Abe K, et al. ER stress-mediated apoptosis in a
811 new mouse model of osteogenesis imperfecta. PLoS Genet. 2008;4(2):e7.
812 39. Forlino A, Kuznetsova NV, Marini JC, Leikin S. Selective retention and degradation of molecules
813 with a single mutant alpha1(I) chain in the Brtl IV mouse model of OI. Matrix Biol. 2007;26(8):604-14.
814 40. Mirigian LS, Makareeva E, Mertz EL, Omari S, Roberts-Pilgrim AM, Oestreich AK, et al.
815 Osteoblast Malfunction Caused by Cell Stress Response to Procollagen Misfolding in alpha2(I)-G610C
816 Mouse Model of Osteogenesis Imperfecta. J Bone Miner Res. 2016;31(8):1608-16.
817 41. Gioia R, Tonelli F, Ceppi I, Biggiogera M, Leikin S, Fisher S, et al. The chaperone activity of 4PBA
818 ameliorates the skeletal phenotype of Chihuahua, a zebrafish model for dominant osteogenesis
819 imperfecta. Hum Mol Genet. 2017;26(15):2897-911.
820 42. Kimura S. Wide distribution of the skin type I collagen alpha 3 chain in bony fish. Comp Biochem
821 Physiol B. 1992;102(2):255-60.
822 43. Exposito JY, Valcourt U, Cluzel C, Lethias C. The fibrillar collagen family. International journal of
823 molecular sciences. 2010;11(2):407-26.
824 44. McBride DJ, Jr., Choe V, Shapiro JR, Brodsky B. Altered collagen structure in mouse tail tendon
825 lacking the alpha 2(I) chain. J Mol Biol. 1997;270(2):275-84.
826 45. Kuznetsova NV, McBride DJ, Leikin S. Changes in thermal stability and microunfolding pattern of
827 collagen helix resulting from the loss of alpha2(I) chain in osteogenesis imperfecta murine. J Mol Biol.
828 2003;331(1):191-200.
829 46. Han S, McBride DJ, Losert W, Leikin S. Segregation of type I collagen homo- and heterotrimers
830 in fibrils. J Mol Biol. 2008;383(1):122-32.
831 47. Ranzoni AM, Corcelli M, Hau KL, Kerns JG, Vanleene M, Shefelbine S, et al. Counteracting bone
832 fragility with human amniotic mesenchymal stem cells. Scientific reports. 2016;6:39656.
833 48. Vanleene M, Saldanha Z, Cloyd KL, Jell G, Bou-Gharios G, Bassett JH, et al. Transplantation of
834 human fetal blood stem cells in the osteogenesis imperfecta mouse leads to improvement in multiscale
835 tissue properties. Blood. 2011;117(3):1053-60.
836 49. Vanleene M, Porter A, Guillot P-V, Boyde A, Oyen M, Shefelbine S. Ultra-structural defects
837 cause low bone matrix stiffness despite high mineralization in osteogenesis imperfecta mice. Bone.
838 2012;50(6):1317-23.
839 50. Bart ZR, Hammond MA, Wallace JM. Multi-scale analysis of bone chemistry, morphology and
840 mechanics in the oim model of osteogenesis imperfecta. Connect Tissue Res. 2014;55 Suppl 1:4-8.
841 51. Miller E, Delos D, Baldini T, Wright TM, Pleshko Camacho N. Abnormal mineral-matrix
842 interactions are a significant contributor to fragility in oim/oim bone. Calcif Tissue Int. 2007;81(3):206-
843 14.
844 52. Zimmerman SM, Heard-Lipsmeyer ME, Dimori M, Thostenson JD, Mannen EM, O'Brien CA, et al.
845 Loss of RANKL in osteocytes dramatically increases cancellous bone mass in the osteogenesis
846 imperfecta mouse (oim). Bone Rep. 2018;9:61-73.
847 53. IMPC. International Mouse Phenotyping Consortium: Col1a2 [Available from:
848 https://www.mousephenotype.org/data/genes/MGI:88468.
849 54. Simon MM, Greenaway S, White JK, Fuchs H, Gailus-Durner V, Wells S, et al. A comparative
850 phenotypic and genomic analysis of C57BL/6J and C57BL/6N mouse strains. Genome Biol.
851 2013;14(7):R82.
852 55. Takigawa S, Frondorf B, Liu S, Liu Y, Li B, Sudo A, et al. Salubrinal improves mechanical
853 properties of the femur in osteogenesis imperfecta mice. J Pharmacol Sci. 2016;132(2):154-61.
854 56. Oganesian A, Au S, Horst JA, Holzhausen LC, Macy AJ, Pace JM, et al. The NH2-terminal
855 propeptide of type I procollagen acts intracellularly to modulate cell function. J Biol Chem.
856 2006;281(50):38507-18.
857 57. Hayata T, Nakamoto T, Ezura Y, Noda M. Ciz, a transcription factor with a nucleocytoplasmic
858 shuttling activity, interacts with C-propeptides of type I collagen. Biochem Biophys Res Commun.
859 2008;368(2):205-10.

58. Marongiu M, Deiana M, Marcia L, Sbardellati A, Asunis I, Meloni A, et al. Novel action of FOXL2 as mediator of Col1a2 gene autoregulation. Dev Biol. 2016;416(1):200-11.
59. Skarnes WC, Rosen B, West AP, Koutsourakis M, Bushell W, Iyer V, et al. A conditional knockout resource for the genome-wide study of mouse gene function. Nature. 2011;474(7351):337-42.
60. Sykes B, Puddle B, Francis M, Smith R. The estimation of two collagens from human dermis by interrupted gel electrophoresis. Biochem Biophys Res Commun. 1976;72(4):1472-80.
61. Schriefer JL, Robling AG, Warden SJ, Fournier AJ, Mason JJ, Turner CH. A comparison of mechanical properties derived from multiple skeletal sites in mice. Journal of biomechanics. 2005;38(3):467-75.
62. van 't Hof RJ, Dall'Ara E. Analysis of Bone Architecture in Rodents Using Micro-Computed Tomography. Methods Mol Biol. 2019;1914:507-31.
63. Phillips CL, Bradley DA, Schlotzhauer CL, Bergfeld M, Libreros-Minotta C, Gawenis LR, et al. Oim mice exhibit altered femur and incisor mineral composition and decreased bone mineral density. Bone. 2000;27(2):219-26.

Supplementary Data

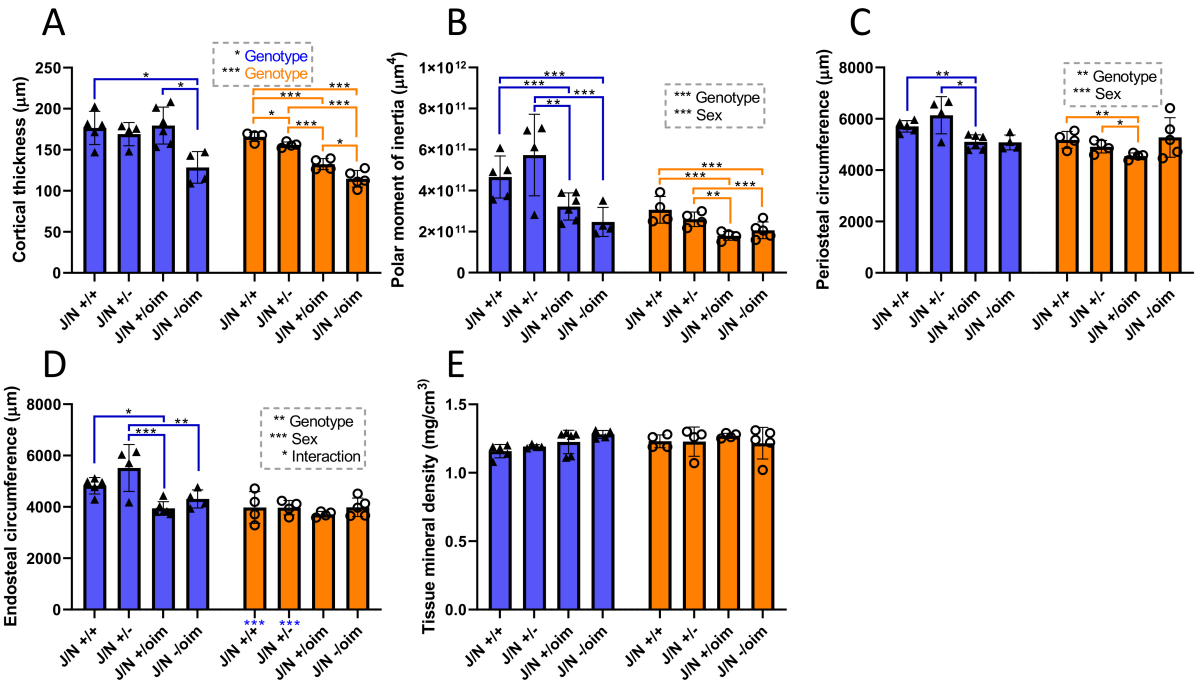

Figure S1. Femoral cortical bone analyses in mixed heterozygotes. MicroCT scans were performed at 8 weeks of age in the crossed oim/Col1a2 null line. Reconstruction and analysis of scan files enabled determination of cortical thickness (A), polar moment of inertia (B), periosteal (C) and endosteal (D) circumference, as well as bone density (E). Blue bars/triangles = males, orange bars/circles = females. Blue and orange brackets show differences between genotypes within males (blue) or females (orange). Male/female differences for particular genotypes are shown below the x-axis for females (blue stars). * p-value < 0.05, ** p-value <0.01 and *** p-value <0.001. n=4 for all groups, except male J/N +/+ and female J/N -/oim where n=5, and male J/N +/oim where n=6.

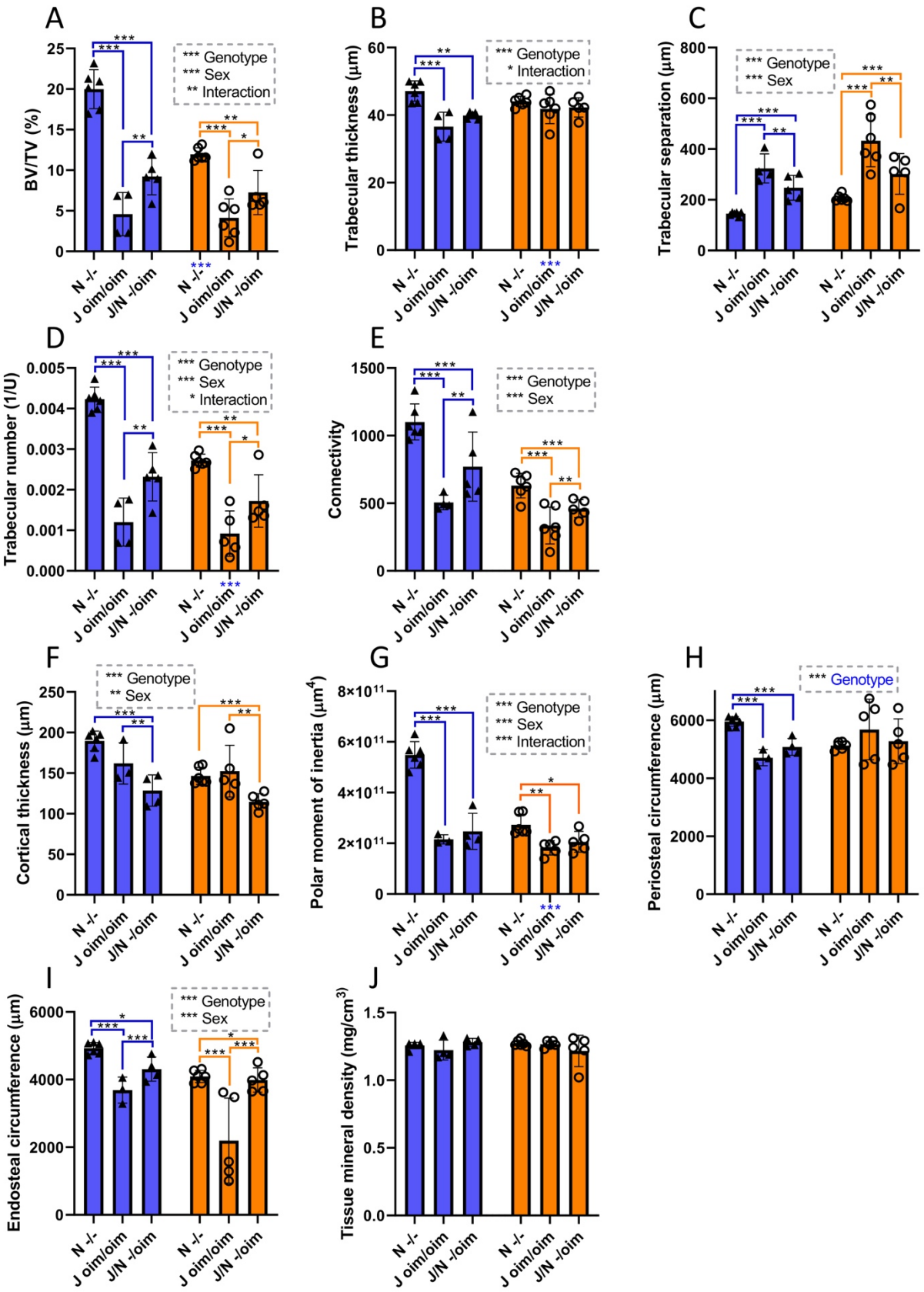

Figure S2. Bone structural properties in compound heterozygotes are generally less severe than in oim homozygotes. Bone volume (A), trabecular thickness (B), trabecular separation (C), trabecular number (D), connectivity (E), cortical thickness (F), polar moment of inertia (G), periosteal (H) and

endosteal (I) circumference, as well as bone density (J) comparisons are shown for Col1a2 null homozygotes (-/-), oim homozygotes (oim/oim) and compound heterozygotes (-/oim). Blue bars/triangles = males, orange bars/circles = females. Blue and orange brackets show differences between genotypes within males (blue) or females (orange). Male/female differences for particular genotypes are shown below the x-axis for females (blue stars). * p-value < 0.05, ** p-value <0.01 and *** p-value <0.001. For trabecular parameters (A-E) n=6 for all groups except -/oim (both sexes) and female oim/oim in D where n=5, and for male oim/oim where n=4. For cortical parameters (F-J) n=6 for -/-, n=5 for female oim/oim and -/oim, whilst n=4 for male -/oim and n=3 for male oim/oim (except in J where n=4 for male oim/oim).